

This discussion paper is/has been under review for the journal Atmospheric Chemistry and Physics (ACP). Please refer to the corresponding final paper in ACP if available.

Saharan and asian dust: similarities and differences determined by CALIPSO, AERONET and a coupled climate-aerosol microphysical model

L. Su and O. B. Toon

Department of Atmospheric and Oceanic Sciences, Laboratory for Atmospheric and Space Physics, University of Colorado, Boulder, Colorado, USA

Received: 23 October 2010 – Accepted: 18 November 2010 – Published: 2 December 2010

Correspondence to: L. Su (sul@colorado.edu)

Published by Copernicus Publications on behalf of the European Geosciences Union.

Saharan and asian dust

L. Su and O. B. Toon

Title Page

Abstract

Introduction

Conclusions

References

Tables

Figures

◀

▶

◀

▶

Back

Close

Full Screen / Esc

Printer-friendly Version

Interactive Discussion



Abstract

This study compares the properties of atmospheric dust from the Saharan deserts and the Asian deserts using data from CALIPSO and AERONET during 2006 and 2007 along with simulations using a coupled climate-microphysical sectional model. Saharan deserts are largely south of 30° N, while Asian ones are primarily north of 30° N, hence they experience different meteorological regimes. Saharan dust lifting occurs all year long, primarily due to subtropical weather systems. However, Asian dust is lifted mostly in spring when mid-latitude frontal systems lead to high winds. Rainfall is more abundant over Asia during the dust lifting events, leading to greater local dust removal than over the Sahara. However, most dust removal is due to sedimentation. Despite the different meteorological regimes, the same dust lifting schemes work in models for Asian and Saharan dust. The magnitudes of dust lifted in Africa and Asia differ significantly over the year. In our model the yearly horizontal dust flux just downwind of the African dust source is about 1446 Tg (10° S–40° N, 10° E) and from the Asian dust source it is about 355 Tg (25° N–55° N, 105° E) in 2007, which is comparable to previous studies. We find the difference in dust flux is mainly due to the larger area over which dust is lifted in Africa than Asia. However, Africa also has stronger winds in some seasons. Once lifted, the Saharan dust layers generally move toward the west and descend in altitude from about 7 km to the surface over several days in the cases studied. Asian dust often has multiple layers (two layers in the cases studied) during transport largely to the east. One layer stays well above boundary layer during transport and shows little descent, while the other, lower, layer descends with time. This observation contrasts with studies suggesting the descent of Saharan dust is due to sedimentation of the particles, and suggests instead it is dominated by meteorology. We find the size distributions of Asian and African dust are similar when the dust is lifted, but the mode size can differ and secondary size modes can develop due to differences in vertical wind velocities during transport. The single scattering albedo of African and Asian dust does differ, due primarily to the imaginary parts of the refractive indexes being different,

Saharan and asian dust

L. Su and O. B. Toon

Title Page

Abstract

Introduction

Conclusions

References

Tables

Figures

◀

▶

◀

▶

Back

Close

Full Screen / Esc

Printer-friendly Version

Interactive Discussion



which in turn is likely due to different dust composition. This study is a step towards a global understanding of dust and its properties.

1 Introduction

Airborne mineral dust is one of the major components of atmospheric aerosols. Dust plays an important role in the atmospheric global circulation (Dunion and Velden, 2004; Wu, 2007), air pollution (Prospero, 1999; VanCuren, 2003), biogeochemical processes (Duce et al., 1991; Martin et al., 1994; Shinn et al., 2000), radiative budget (Sokolik and Toon, 1996; Kaufman et al., 2001), and human health (IPCC, 2007). Dust varies over short time scales and geologic time (Rea et al., 1985).

The Saharan desert is the largest and most continuous dust source in the world. Saharan dust can be transported across the tropical North Atlantic and into the Caribbean region as well as into Europe (Prospero and Carlson, 1972; Prospero, 1996; Colarco et al., 2002, 2003a,b; Toon, 2003; Liu et al., 2008; Generoso et al., 2008). Especially in summer large amounts of Saharan dust are transported across the Atlantic Ocean, which is dominated by the Azores High, and arrive in the Caribbean Sea (Doherty et al., 2008).

The Taklimakan and Gobi deserts are the major dust sources in Asia (Uno et al., 2005). Asian dust can be transported over the North Pacific Ocean and reach Midway and North America (Duce et al., 1980; Shaw, 1980; Betzer et al., 1988; Clarke et al., 2001; Husar et al., 2001; Tratt et al., 2001; Huang et al., 2008; Eguchi et al., 2009; Su and Toon, 2009). Asian dust also can be transported over global scales (Clarke et al., 2001; Grousset et al., 2003; Uno et al., 2009).

Recently, special attention has been paid to Saharan dust in field campaigns such as the Puerto Rico Dust Experiment (PRIDE) (Reid et al., 2002, 2003b; Maring et al., 2003; Colarco et al., 2003a,b), the Dust And Biomass EXperiment (DABEX) (Osborne et al., 2008), the SAharian Mineral dUst experiMent (SAMUM) (Heintzenberg, 2008; Knippertz et al., 2008; Muller et al., 2008), the African Monsoon Multidisciplinary

Saharan and asian dust

L. Su and O. B. Toon

Title Page

Abstract

Introduction

Conclusions

References

Tables

Figures

◀

▶

◀

▶

Back

Close

Full Screen / Esc

Printer-friendly Version

Interactive Discussion



Saharan and asian dust

L. Su and O. B. Toon

[Title Page](#)[Abstract](#)[Introduction](#)[Conclusions](#)[References](#)[Tables](#)[Figures](#)[◀](#)[▶](#)[◀](#)[▶](#)[Back](#)[Close](#)[Full Screen / Esc](#)[Printer-friendly Version](#)[Interactive Discussion](#)

Analysis (AMMA) (Rajot et al., 2008; Heese and Wiegner, 2008; Haywood et al., 2008), and the GERB Intercomparison of Longwave and Shortwave radiation (GERBILS) (Haywood et al., 2005; Marsham et al., 2008). Saharan dust has been studied through model simulations (Marticorena et al., 1997; Colarco et al., 2002, 2003a,b; Maring et al., 2003; Liu et al., 2008; Generoso et al., 2008), and satellite retrievals (Liu et al., 2008; Liu, Z. et al., 2008; Generoso et al., 2008; Cuesta et al., 2009).

Several field campaigns have been also conducted regarding Asian dust aerosols including the Aerosol Characterization Experiments (ACE-Asia) (Huebert et al., 2003; Seinfeld et al., 2004), the Indian Ocean Experiment (INDOEX) (Ramanathan et al., 2001, Rasch et al., 2001), the TRANsport and Chemical Evolution over the Pacific experiment (TRACE-P) (Carmichael et al., 2003; Jacob et al., 2003), the Intercontinental Chemical Transport Experiment Phase B (INTEX-B) (Arellano et al., 2007; McKendry et al., 2008), and the PACific Dust EXperiment (PACDEX) (Stith et al., 2008). Asian dust also has been investigated through model simulations (Tegen and Fung, 1994; Schulz et al., 1998; Mahowald et al., 1999, 2006; Ginoux et al., 2001; Uno et al., 2002, 2004, 2008, 2009; Carmichael et al., 2003; Chin et al., 2003, 2004; Gong et al., 2003; Zender et al., 2003a; Shimizu et al., 2004; Shao and Dong, 2006; Huang et al., 2009; Su and Toon, 2009), and satellite retrievals (Huang et al., 2007, 2008; Liu et al., 2008; Uno et al., 2008).

Most studies have focused on either Saharan dust or Asian dust. Here we investigate the differences and similarities in dust lifting, dust removal processes, seasonal variations, transport mechanisms, and physical properties between Saharan dust and Asian dust using satellite data such as CALIPSO, ground-based data such as AERONET, and numerical models.

Numerous satellite observations have been made of Saharan and Asian dust. Here we focus on data from the Cloud-Aerosol Lidar and Infrared Pathfinder Satellite Observation (CALIPSO). CALIPSO was launched in April 2006 (Liu et al., 2006; Winker et al., 2007). The Cloud-Aerosol Lidar with Orthogonal Polarization (CALIOP), on CALIPSO, is a two-wavelength (532 and 1064 nm), polarization-sensitive (at 532 nm) instrument.

CALIOP provides substantial and unique information on vertical and geographical distributions of clouds and aerosols. CALIOP conducts nearly continuous observations of height-resolved attenuated backscatter over the globe (Sassen, 2000; Winker et al., 2003).

5 The Aerosol Robotic NETwork (AERONET) is a globally distributed remote sensing aerosol-monitoring network of ground-based sun photometers that measure sun and sky radiances in 16 spectral channels (340–1640 nm) (Holben et al., 1998). AERONET provides observations of aerosol optical depth (AOD), inversion products such as size distribution and single scattering albedo, and precipitable water. We use the cloud-
10 screened and quality-assured AERONET Level 2.0 data in this study (Smirnov et al., 2000).

Numerical modeling of dust aerosols is essential for climate studies, and to better understand the behavior of the dust aerosols in the atmosphere. We use a coupled three-dimensional climate-microphysical sectional model, which is capable of simulat-
15 ing the mineral dust aerosols (Su and Toon, 2009) to explore the differences between atmospheric dust from the Saharan deserts and from the Asian deserts.

The various observations and models have led to a number of questions about Asian and African dust. It is clear from satellite observations that the dust optical depth is generally larger over the Atlantic, than over the Pacific. Is this difference due to
20 more dust being lifted over Africa, to more dust being removed over the Pacific, to seasonality in dust lifting, or to other factors? Is the size distribution of dust downwind of African or Asian dust sources different, or the same so that it can be modeled using the same dust source functions? Are the dust optical properties different between Asian and African dust, and if so are the differences related to dust composition, or
25 to particle size? Do the same mechanisms control dust transport in the two regions of the world? For instance, Saharan dust is observed to descend when crossing the Atlantic. Is this descent due to sedimentation, so Asian dust should also descend, or to air motions which may differ? Does the different meteorology of Africa and Asia lead to differences in the vertical distribution of the two types of dust? We seek to answer

Saharan and asian dust

L. Su and O. B. Toon

Title Page

Abstract

Introduction

Conclusions

References

Tables

Figures

◀

▶

◀

▶

Back

Close

Full Screen / Esc

Printer-friendly Version

Interactive Discussion



these questions here.

Section 2 of this paper describes our three-dimensional coupled model configuration and the dust emission scheme. Section 3 evaluates the model results and provides comparisons with observations for seasonal and geographic variation in dust lifting and removal, for geographic differences in dust vertical distributions, for dust size distributions, and for dust optical properties. Section 4 presents a summary and conclusions.

2 Model description

The three-dimensional coupled climate-aerosol microphysical model based on the NCAR Community Atmosphere Model (CAM3) (Collins et al., 2004) and the University of Colorado/NASA Community Aerosol and Radiation Model for Atmospheres (CARMA2.3) (Toon et al., 1988; Jensen et al., 1994; Ackerman et al., 1995) is a new numerical model that has been described in detail by Su and Toon (2009). The coupled model we are using for the Saharan and Asian dust simulations includes a three-dimensional climate model (CAM3) and an aerosol microphysical sectional model (CARMA2.3). CAM3 is driven by off-line meteorological fields from NCAR and the National Center for Environmental Prediction (NCEP) reanalysis package (Rasch et al., 1997). We treat CARMA2.3 as a bin-resolved column aerosol-microphysical sectional model that has the same domain as CAM3. We also choose the finite-volume (FV) dynamical core for the dynamical equations of CAM3 to conserve the mass for tracers as discussed by Lin and Rood (1996). The coupled CAM3/CARMA2.3 model includes dust sources, transport, removal processes, and optical properties of dust aerosols (Su and Toon, 2009).

We configured the coupled CAM3/CARMA2.3 model with a horizontal resolution of $2^\circ \times 2.5^\circ$ degrees, and 28 hybrid vertical model layers from the surface to about 40 km. We used 16 dust size bins with central radius covering the range from 0.1 to $10 \mu\text{m}$ to parameterize the modified Ginoux et al. (2001) dust source function as discussed in Su and Toon (2009). Briefly, the dust lifting is physically driven by the surface stress based

Saharan and asian dust

L. Su and O. B. Toon

Title Page

Abstract

Introduction

Conclusions

References

Tables

Figures

◀

▶

◀

▶

Back

Close

Full Screen / Esc

Printer-friendly Version

Interactive Discussion



Saharan and asian dust

L. Su and O. B. Toon

[Title Page](#)[Abstract](#)[Introduction](#)[Conclusions](#)[References](#)[Tables](#)[Figures](#)[◀](#)[▶](#)[◀](#)[▶](#)[Back](#)[Close](#)[Full Screen / Esc](#)[Printer-friendly Version](#)[Interactive Discussion](#)

on the saltation-sandblasting process (Gomes et al., 1990; Shao and Raupach, 1993; Shao and Lu, 2000; Su and Toon, 2009). We use the friction wind velocity in the dust source function based on the atmospheric stability and land surface conditions (e.g. surface roughness length). We also account for the recently detected desertification in Inner Mongolia in the dust erodibility source factor (Chin et al., 2003, 2004; P. Ginoux, personal communication, 2007; Su and Toon, 2009). The Weibull wind distribution that represents the subgrid-scale velocity distribution has been implemented in the dust-lifting scheme to better represent the dust lifting process by subgrid scale winds that are not represented well due to the coarse resolution of global models (Gillette and Passi, 1988; Su and Toon, 2009).

We use the same parameterization of removal processes (wet deposition and dry deposition) as described in Su and Toon (2009). Dust aerosols are scavenged both by rain and snow including below-cloud and in-cloud scavenging for each model layer in a manner that is size and composition independent (Barth et al., 2000; Rasch et al., 2001; Su and Toon, 2009). The dry deposition includes sedimentation near the surface (which dominates for coarse mode particles) and turbulent mix-out (which dominates for fine mode particles). The sedimentation fall velocities are calculated in CARMA2.3 by Stokes law at low Reynold's number ($Re < 1$). Corrections are made at high Reynold's numbers ($Re > 1$) based on Prupacher and Klett (1997). We modified the dry deposition scheme following Marticorena and Bergametti (1995) and Ginoux et al. (2001) to account for both the bin-resolved dust particles and the effect of soil moisture on dust lifting (Su and Toon, 2009).

3 Results

3.1 Comparison of dust abundance and fluxes over the Atlantic and Pacific, and seasonal variations

Here we address the problem of why the optical depths of dust over the Pacific and Atlantic are so different. Figure 1 shows the daily-averaged and column-integrated spectral optical depth at 500 nm at Osaka in the Pacific in May 2007 (top) and at Capo Verde in the Atlantic in July 2007 (bottom) both from our model and from AERONET data. In general, the optical depth is higher over the Atlantic at Capo Verde than over Pacific at Osaka at similar downwind distances from the two dust sources even during the primary months of dust storm activity (such as May in Asia and July in the Sahara). The monthly-averaged optical depth is 0.382 and 0.339 over Pacific at Osaka in May 2007 for AERONET data and the model simulation, respectively. However, the monthly-averaged optical depth is 0.613 and 0.579 over Atlantic at Capo Verde in July 2007 for AERONET data and model simulation, respectively.

The dust fluxes into the two ocean basins tell a similar story to the one told by the optical depths. Figure 2 shows the modeled dust fluxes in 2007 from 10° S–40° N latitude across four different longitude planes at 10° E, 35° W, 80° W, and 125° W. Figure 3 shows the map used in this study for Saharan dust. The dashed lines denote the four longitude planes (10° E, 35° W, 80° W, and 125° W) and the latitude boundaries (10° S to 40° N) at which dust fluxes were computed. We choose the latitude range between 10° S to 40° N based on previous studies using the GEOS-Chem model and CALIPSO analysis (Generoso et al., 2008; Liu et al., 2008b) suggesting that most Saharan dust plumes occurred and were transported downwind within this area. These longitudes span the distance from the Saharan dust source regions, across the Atlantic, over the Caribbean and into the Pacific. The dust flux (orange dashed line in Fig. 2) crossing the 10° E plane (10° S–40° N) at the western edge of the Saharan Desert is about 100 Tg for each month and is about 120 Tg per summer month when the flux is greatest. The annual flux is about 1446.61 Tg across the 10° E plane in 2007 (orange dashed line in

Saharan and asian dust

L. Su and O. B. Toon

Title Page

Abstract

Introduction

Conclusions

References

Tables

Figures

◀

▶

◀

▶

Back

Close

Full Screen / Esc

Printer-friendly Version

Interactive Discussion



Fig. 2). This is about 94% of the total amount of Saharan dust (1539.36 Tg) lifted in the model for the year. The other 6% of the dust (92.75 Tg) goes north toward Europe in the model.

The Saharan Desert is located in the tropics and sub-tropics, and usually experiences deep convection throughout the year. The dust outbreaks are contained in a deep mixed layer, referred to as the Saharan Air Layer (SAL). The SAL usually extends to 5–6 km or higher in altitude over the Saharan Deserts due to the strong solar heating (Prospero et al., 1972 and 1981; Karyampudi et al., 1999; Colarco et al., 2003b). Strong winds embedded in the tropical trades (northeasterly flow) continually lift dust from the surface of Saharan Deserts. The annual dust cycle of the African dust sources can be triggered and modulated by synoptic systems, such as African easterly waves in the Atlantic region (Prospero and Carson, 1972; Westphal et al., 1987; Jones et al., 2003). The dust outbreaks usually occur in the ridge of passing easterly waves with a period of 5–7 days (Prospero and Carson, 1972). The African easterly waves are identified through filtered (2.5–10 days) relative vorticity at 700 hPa over the tropical Atlantic Ocean. About 20% of the dust entrainment into the atmosphere is related to easterly wave activity, and approximately 10%–20% of the seasonal variation of Saharan Desert dust transported across the North Atlantic Ocean is regulated by easterly waves (Jones et al., 2003).

Figures 2 and 4 show that about 90% of the dust is removed by the time it reaches 35° W. During most months of the year only about 1% of the dust reaches as far as 80° W, the longitude of Cuba. However, in the summer of 2007 our model indicates a relatively larger dust flux (around 2.5 Tg/month, 4.7% of total dust flux) reached the Caribbean Sea (the 80° W plane red curve in Fig. 2). These dust fluxes are qualitatively consistent with some previous studies. Colarco et al. (2003b) and Doherty et al. (2008) indicate each summer large amounts of Saharan dust are transported across the Atlantic Ocean and arrive in Caribbean Sea. The Saharan dust transport into the Caribbean is controlled primarily by a semi-permanent high, the Azores High (also called North Atlantic High), which usually extends westward toward Bermuda. This

Saharan and asian dust

L. Su and O. B. Toon

[Title Page](#)[Abstract](#)[Introduction](#)[Conclusions](#)[References](#)[Tables](#)[Figures](#)[◀](#)[▶](#)[◀](#)[▶](#)[Back](#)[Close](#)[Full Screen / Esc](#)[Printer-friendly Version](#)[Interactive Discussion](#)

anticyclone becomes stronger and moves north in summer, and it moves south and becomes weaker in winter. The longitudinal displacement of the Azores High is highly related to the Saharan dust transport into Caribbean.

Figure 2 also shows that the far-most plane over the Pacific at 125° W (the asterisk marked dash-line) has nearly the same dust flux values as the 80° W plane in many months such as February, April, October, and December. However, in the months of June, July and August, there is a significant loss of dust between 80° W and 125° W. The amount of loss in this longitude region is related to the position of the Inter-tropical Convergence Zone (ITCZ). During summer the ITCZ moves into latitudes near 10° N, and there is significant convection over Central America due to the frontal zone of the ITCZ bringing the warm, moist air from the Gulf of Guinea into the hot, dry Saharan air to the north. This convection is quite efficient at removing the dust (Pfister et al, 2010). However, during other parts of the year there is less convection over Central America and our model suggests that dust is more likely to reach the Pacific.

Figure 4 presents the modeled monthly dust flux between 10° S to 40° N for 2007 at various longitudes as a fraction of the flux at 10° E. The 35° W to 10° E ratio shows a monthly variation that may be related to the position of the Azores High as we discussed earlier. Generoso et al. (2008) estimated 151 Tg of dust was deposited in 2006 in the area bounded by 5° N–27° N and 17° W–100° W. We similarly find that total annual dust deposition in the tropical Atlantic in the area bounded by 5° N–30° N and 17° W–100° W is about 163 Tg in 2007.

Figure 5 shows the modeled annual dust wet deposition between 10° S to 40° N for 10° E–35° W, 35° W–80° W, and 80° W–125° W for Saharan dust in 2007. The annual total of the dust wet deposition over 10° S to 40° N and 10° E to 125° W is 163.30 Tg based on the model simulations. Over the year there are about total 146.45 Tg (10% of total annual dust flux of 1446.61 Tg crossing the 10° E plane), 16.38 Tg (10% of total annual dust flux of 161.54 Tg crossing the 35° W plane), and 0.47 Tg (3% of total annual dust flux of 15.29 Tg crossing the 80° W plane) of dust removed during transport between 10° E and 35° W, 35° W and 80° W, 80° W and 125° W, respectively, by wet

Saharan and asian dust

L. Su and O. B. Toon

[Title Page](#)[Abstract](#)[Introduction](#)[Conclusions](#)[References](#)[Tables](#)[Figures](#)[◀](#)[▶](#)[◀](#)[▶](#)[Back](#)[Close](#)[Full Screen / Esc](#)[Printer-friendly Version](#)[Interactive Discussion](#)

deposition. Therefore the results of our model simulation indicate that 10% of total dust crossing 10° E is deposited before it reaches the 125° W plane in 2007 by wet removal, of which about 60% of the wet deposition occurs in summer. There is less wet deposition in spring and autumn. Our study suggests that the wet removal process is a minor contributor to the total dust loss over the Atlantic (see Table 1).

Figure 6 shows the modeled annual dust fluxes (between 25° N–55° N) across different longitude planes (105° E, 150° E, 195° E, and 240° E) for Asian dust in 2007. Figure 7 shows the map used in this study for Asian dust. The dashed lines denote the four longitude planes (105° E, 150° E, 195° E, and 240° E) and the latitude boundaries (25° N to 55° N). We chose the latitude range between 25° N to 55° N based on previous modeling and observational studies showing that most Asian dust plumes occurred and were transported downwind within this area (Eguchi et al., 2003 and 2009; Huang et al., 2008). The total dust flux (orange dashed line in Fig. 6) across the 105° E plane, which crosses central Mongolia in the Asian deserts, is 355 Tg in 2007. Figure 2 showed an annual dust flux across 10° E from the Sahara of about 1446 Tg in 2007. Therefore, about 4 times as much dust was transported downwind of the Sahara desert in 2007, as downwind of the Asian deserts. Unlike the case for the Sahara, there is a strong seasonal variation in Asian dust fluxes. We find that 62% of the 355 Tg lifted is generated in the months March–June. Eguchi et al. (2003) reported that the dust transported through the longitudinal cross-plane at 90° E is approximately 34.1 Tg for a period of 5–15 May 2007 based on a 3-D aerosol model. Our model estimates about 36.4 Tg within the same latitude region between 25° N–55° N.

The seasonal variation of dust outbreaks is associated with variation in the wind speed (Shao and Dong, 2006), the surface vegetation (Lee and Sohn, 2009), and the soil moisture and snow cover (Laurent et al., 2006). Strong winds occur most frequently in spring in Asia due to the activity of mid-latitude frontal systems. The mid-latitude cyclones associated with intense cold fronts from Mongolia to northeastern China not only generate dust storms, but also lift Asian dust into the westerly jet in the free atmosphere. There is no equivalent of the SAL over Asia, though some of the dust

Saharan and asian dust

L. Su and O. B. Toon

Title Page

Abstract

Introduction

Conclusions

References

Tables

Figures

◀

▶

◀

▶

Back

Close

Full Screen / Esc

Printer-friendly Version

Interactive Discussion



is transported in a relatively shallow boundary layer. Deep dry convection is a major feature of Saharan Deserts (Cuesta et al., 2009). The mixed boundary layer depth and the tropopause altitude above the low-latitude tropical surface of Africa are higher than at mid-latitudes in Asia. Thus the springtime weather in Asia produces intense dust storm events in which dust is transported along the direction of the westerly winds. However, this transport is not associated with a deep convective boundary layer, as it is for Saharan dust.

The dust emission over the Asian dust source regions is substantially suppressed after spring not only due to the weaker Mongolian cyclonic activity but also because of the increasing vegetation (Lee and Sohn, 2009). Laurent et al. (2006) indicates that the soil moisture and snow cover in the northern deserts of China decreases the dust emission by 94% and 84%, respectively, in winter but the dust emissions of Taklimakan desert are not noticeably influenced by the soil moisture and snow cover due to low precipitation and snow falls.

Figure 8 presents the monthly dust flux between 25° N to 55° N latitude across 240° E and 150° E longitudes as a fraction of the flux across 105° E. Figure 8 shows that only about 10% of the dust lifted reaches the longitude of Japan (150° E) and only 5% reaches the West coast of the US (240° E). This large mass loss suggests that the removal processes (including wet and dry deposition) play an essential role during the Asian dust transport to 150° E. Like Sahara dust there is a low layer of Asian dust that is rapidly removed by deposition. However, the relatively small dust particles lifted from the dust source that are entrained into air at high altitude (up to 10 km) can be transported via upper tropospheric westerly jets over long distance as has been pointed out from observations by Stith et al. (2009). Once dust passes Japan, removal is less important. Eguchi et al. (2009) reported that about 30% of dust crossing 140° E is transported eastward and arrives in the North America based on the CALIPSO and SPRINTARS model analysis, which is consistent with our model simulations of 40% of Asian dust crossing 150° E reaching the west coast of America.

Saharan and asian dust

L. Su and O. B. Toon

Title Page

Abstract

Introduction

Conclusions

References

Tables

Figures

I◀

▶I

◀

▶

Back

Close

Full Screen / Esc

Printer-friendly Version

Interactive Discussion



Saharan and asian dust

L. Su and O. B. Toon

[Title Page](#)[Abstract](#)[Introduction](#)[Conclusions](#)[References](#)[Tables](#)[Figures](#)[◀](#)[▶](#)[◀](#)[▶](#)[Back](#)[Close](#)[Full Screen / Esc](#)[Printer-friendly Version](#)[Interactive Discussion](#)

The dust flux ratios in Fig. 8 are lowest in the months from December to May. This seasonal variability means there is preferential dust removal during the same period when dust is lifted over Asian deserts. This overlap occurs because the low pressure centers over the Asian deserts are not only responsible for the strong winds needed for the dust lifting, but also act as sources of rain needed for dust removal. This is a different phenomenon than for Sahara dust.

Figure 9 shows the modeled annual dust wet deposition between 25° N to 55° N for 105° E to 150° E, 150° E to 195° E, and 195° E to 240° E for Asian dust in 2007. The dust flux is correlated with the wet removal. In part this is because the same systems that lift the dust, bring rain. About 52 Tg (15% of dust crossing the 105° E plane) of dust is removed during transport from 105° E to 150° E by wet deposition on an annual average. The results of our model simulation indicate that more dust is wet deposited during spring and summer, than in autumn and winter. This study also suggests that wet removal process plays a larger role in dust removal for Asian dust (15% of dust crossing the 105° E plane) than Saharan dust (10% of dust crossing the 10° E plane). This larger loss is due to the abundant rainfall over Asia (especially in spring and summer) leading to greater local dust removal than over the Sahara.

The dust mass flux from the Sahara in 2007 is about 4 times greater than that from Asia across a plane that is 45 degrees longitude from the source. Table 1 shows the factors that contribute to the differences of the total dust fluxes between Asian dust and Saharan dust as simulated from the coupled CAM3.0/CARMA2.3 model in year 2007. We can see the wet and dry deposition processes have similar magnitudes for Asian and Saharan dust. Although most of the dust is removed in transport over these distances, deposition is not the major mechanism causing the differences in the total dust fluxes between the two dust sources. The soil erodibility factor is not a function of time in the model. There are the similar values of the area averaged soil erodibility factor (0.078 for Asian deserts and 0.081 for Saharan deserts). The total areas of the dust sources are $2.07 \times 10^6 \text{ km}^2$ and $8.95 \times 10^6 \text{ km}^2$ for Asian deserts and Saharan deserts, respectively. However, the annual averaged areas over which dust lifting

occurs (when wind exceeds the threshold velocity, which is related to the particle size distribution and soil moisture) are $1.33 \times 10^6 \text{ km}^2$ and $4.17 \times 10^6 \text{ km}^2$ for Asian deserts and Saharan deserts, respectively, based on the model simulations. The areas over which dust lifting occurs in various seasons in Saharan deserts are $3.97 \times 10^6 \text{ km}^2$ (spring), $4.53 \times 10^6 \text{ km}^2$ (summer), $4.25 \times 10^6 \text{ km}^2$ (fall), and $3.94 \times 10^6 \text{ km}^2$ (winter). The areas over the Asian deserts are $1.67 \times 10^6 \text{ km}^2$ (spring), $1.15 \times 10^6 \text{ km}^2$ (summer), $1.20 \times 10^6 \text{ km}^2$ (fall), and $1.31 \times 10^6 \text{ km}^2$ (winter). Therefore the different areas over which dust is lifted contributes about a factor of 3 to the difference in total dust lifting between the two sources in 2007. A factor of three is also about the difference in the spring and summer lifting between the Sahara and Asia, so that the area over which dust is lifted dominates the difference between the amounts of dust lifted. We also calculated the seasonal mean power-averaged wind over the dust lifting areas. The power in the wind is directly proportional to the amount of dust lifted in the source function. The values of the power-averaged winds are 4.9 m/s (spring), 5.5 m/s (summer), 5.3 m/s (fall), and 4.7 m/s (winter) for Saharan deserts. And the values of the power-averaged winds are 4.9 m/s (spring), 3.6 m/s (summer), 4.0 m/s (fall), and 4.3 m/s (winter) for Asian deserts. So the annual-averaged and power averaged winds for Asian deserts and Saharan deserts are 4.2 m/s and 5.1 m/s, respectively. The wind speeds are the same between the Sahara and Asia in the spring, so when Asia has most of its dust events it is the area of the source that dominates the difference between Asian and African dust fluxes. However in other times of the year low winds speeds cause Asia to be a less important dust source. Over the year, wind speed contributes about a factor of 1.7 (the lifting depends on the third power of the wind) to the differences of the total dust fluxes between the African and Asian sources. Soil moisture and snow can be seen as restricting the area of the dust sources, or the magnitude of the dust lifting. The soil moisture (the volumetric soil water in the model) is different between the two sources with an annual mean value of $0.1 \text{ mm}^3/\text{mm}^3$ for Asian deserts and $0.03 \text{ mm}^3/\text{mm}^3$ for Saharan deserts (Table 1). The dust flux is not linearly proportional to the soil moisture so soil moisture contributes about a factor of 10% to

Saharan and asian dust

L. Su and O. B. Toon

[Title Page](#)[Abstract](#)[Introduction](#)[Conclusions](#)[References](#)[Tables](#)[Figures](#)[◀](#)[▶](#)[◀](#)[▶](#)[Back](#)[Close](#)[Full Screen / Esc](#)[Printer-friendly Version](#)[Interactive Discussion](#)

the total dust flux differences between the two sources. Other factors that affect the dust flux differences between the two sources can be snow and vegetation (the annual mean snow is 2.5×10^{-5} mm/s over Asian deserts and it is around zero for Saharan deserts in 2007 in the model). Snow and vegetation limit the area of dust lifting, not the magnitudes of dust lifting in our model.

3.2 Dust vertical distribution

We would like to know if Asian and African dust has the same vertical distribution, and to understand how the vertical distribution of dust impacts the downwind transport and properties of dust. As we noted in the previous section the removal over 45 degrees of longitude is similar for Africa and Asia. However, because these are at different latitudes, the times to go these distances are shorter by about 20% for the Asian dust, assuming the wind speeds are similar. However, the mean wind speed at 30° N– 50° N latitude is higher than at 10° N– 30° N latitude, so in fact the Asian dust is traveling faster than the Saharan dust and so has even less time to be removed, by a factor of 1.25 considering distance and wind speed than the African dust. We compare the vertical distribution of Saharan dust with that of Asian dust and explore how each evolves downwind of their respective source. We use data from the CALIOP instrument on CALIPSO for this comparison.

We investigated a case study of dust transport for Saharan dust and one for Asian dust. Over the tropical and subtropical regions the cloud coverage is very high, which makes it hard to acquire enough cloud-free profiles to create case studies. Due to the availability of CALIPSO measurements, we take 17 August to 28 August of 2006 as an example of Saharan dust, and 7 May to 10 May of 2007 as an example of Asian dust.

CALIPSO profile level 1B data contains measurements of Total Attenuated Backscatter at 532 nm (TAB_532) and of Perpendicular Attenuated Backscatter at 532 nm (PAB_532). Following Fernald et al. (1972 and 1984), Young et al. (2008), Liu et al. (2008b), and Cuesta et al. (2009), the dust vertical extinction (km^{-1}) at 532 nm

Saharan and asian dust

L. Su and O. B. Toon

Title Page

Abstract

Introduction

Conclusions

References

Tables

Figures

◀

▶

◀

▶

Back

Close

Full Screen / Esc

Printer-friendly Version

Interactive Discussion



can be calculated by

$$\beta_{532} = \frac{\beta_{532t} \times \delta_{532}}{\exp(-2 \times \beta_{532} \times \nabla z)} \quad (1)$$

Where β_{532t} is the total attenuated backscatter at 532nm ($\text{km}^{-1}\text{sr}^{-1}$), β_{532} is the vertical extinction (km^{-1}), δ_{532} is the lidar ratio (44 for this study based on Liu et al., 2006), and ∇z is the detected layer height. We also screen out the cloud from CALIPSO profile level 1B data based on the CALIPSO cloud layer level 2 data based on Liu et al. (2008b). Nighttime CALIPSO measurements primarily are used in this study because they have less noise. However we use the daytime data for 25 August and 28 because the nighttime data are not available. We expect additional solar background noise in measurements on these two days.

Figure 3 shows the map of CALIPSO tracks for Saharan dust used in this study (17 August to 28 August of 2006). The asterisks indicate the dust transport path for Saharan Deserts from 17 August (most easterly asterisk) to 28 August (most westerly asterisk) of 2006. It should be noted that there are two dust plumes on 17 August of 2006 (as two asterisks denoted), which merged together before it begins its long-range transport across the Atlantic on 18 August of 2006. We averaged these two profiles on 17 August. We used the Hybrid Single-Particle Lagrangian Integrated Trajectory (HYSPLIT) model (Draxler and Rolph, 2003) (<http://www.arl.noaa.gov>) to trace the downwind evolution of Saharan and Asian dust. The HYSPLIT model can be configured to compute air parcel trajectories for complex dispersion and deposition simulations based on the wind fields from the National Center for Environmental Prediction (NCEP) analyses. We averaged the CALIPSO data every 120-laser shots over about 40 km along the track around the regions marked by asterisks. Figure 10 presents the results of the comparison of the vertical distribution (extinction at 532 nm) of Saharan dust between the model (solid marked lines) and CALIPSO data (dashed lines) from 17 August to 28 August of 2006. The simulated dust vertical distribution of Sahara dust is generally consistent with CALIPSO (lidar) retrievals. However, on some days, such

Saharan and asian dust

L. Su and O. B. Toon

Title Page

Abstract

Introduction

Conclusions

References

Tables

Figures

◀

▶

◀

▶

Back

Close

Full Screen / Esc

Printer-friendly Version

Interactive Discussion



Saharan and asian dust

L. Su and O. B. Toon

[Title Page](#)[Abstract](#)[Introduction](#)[Conclusions](#)[References](#)[Tables](#)[Figures](#)[◀](#)[▶](#)[◀](#)[▶](#)[Back](#)[Close](#)[Full Screen / Esc](#)[Printer-friendly Version](#)[Interactive Discussion](#)

as from 19 August to 23 August the model does not capture the sharp layer top that is observed by CALIPSO. Probably the model lacks enough vertical resolution to fully resolve the layer top. However, it is also possible that the upper parts of the layer have been advected horizontally away from the lower parts and the model has not properly captured that transport. The Sahara dust layers descend over time with the top altitude starting at about 7 km on 17 August and reaching the marine boundary layer on 28 August. The typical magnitude of the vertical extinction (vertical average through the dust layer) decreases from 0.023 km^{-1} (averaged from the CALIPSO data) and 0.027 km^{-1} (averaged from the model) on 17 August to 0.01 km^{-1} (averaged from the CALIPSO data) and 0.007 km^{-1} (averaged from the model) on August 28. The dust resides in a well-mixed layer about 2 km thick (between 1 to 3 km in altitude) as it advects west and enters the Caribbean Sea on 23 August. Colarco et al. (2003b) found a similar layer over the Caribbean but located between 3 to 5 km in altitude during the Puerto Rico Dust Experiment (June–July 2000).

The descent of the Saharan dust layers during transport was recognized previously by Colarco et al. (2003b) who suggested it was due partly to particle sedimentation. On the other hand, Doherty et al. (2008) suggested the descent is dominated by vertical air motions. The Sahara Air Layer (SAL) is affected by the Azores High. The Azores High usually extends westward from the Azores toward Bermuda. It becomes stronger and moves north toward the Iberian Peninsula in summer. Descending air in the Azores High will cause the top of the SAL to decline in altitude as air is transported to the Caribbean Sea from West Africa. The transport of dust in the SAL from West Africa to the Caribbean Sea took about one week (17 August to 25 August). The mean vertical velocity of the dust descent is about 6.3 mm/s based on the vertical extinction profiles of 17 August to 25 August 2006. Liu et al. (2008b) found that the mean descending velocity of the top of the Saharan dust layer is about 6 mm/s for transport from the west coast of Africa to the Caribbean Sea based on depolarization profiles for these same days in August 2006. The HYSPLIT model showed that the SAL descended between West Africa and the Caribbean Sea from 17 August to 25 August at about

4.3 mm/s. The difference between the dust descent rate (6.3 mm/s) and the air descent rate (4.3 mm/s) is consistent with the fall velocity of dust particles around 2 μm in size. Hence about one third of the descent rate of the dust is due to sedimentation and two thirds to the descent of the air in the case studied.

5 Figure 7 shows the map of CALIPSO tracks for Asian dust used in this study (7 May (most westerly track) to 10 May (most easterly track) of 2007). The asterisk and the cross marks indicate two dust transport paths for Asian dust from 7 May to 10 May of 2007. We averaged 120-laser shots from CALIPSO over about 40 km along the track both at the asterisk and cross mark points. The paths differ by the altitude of the dust
10 layer. The track to the south was followed by dust below 3 km, and the track to the north by dust above 3 km. The transport paths are tracked by the HYSPLIT model. Vertical shear of the wind prevented a “SAL-like” layer from advecting away from the dust source.

The simulated dust vertical distribution of Asian dust is consistent with CALIPSO (lidar) retrievals (Fig. 11). Asian dust shows multiple layers (two layers in the case
15 studied) during transport. One layer is at the altitudes between about 4.5–6.5 km (and is located to the north along the asterisks in Fig. 13) and shows little descent, while the other, lower layer top descends with time from 3 km on 7 May to 1 km on 9 May (there are no data available below 1 km on 10 May 2007). The HYSPLIT model showed that
20 the air between 4.5–6.5 km ascended at about 0.4 mm/s during transport from 7 May to 10 May of 2007 along the CALIPSO tracks. Such ascent is enough to compensate for the sedimentation of particles as large as 3–4 μm . This ascent is consistent with the mid-latitude frontal cyclones, which not only generate dust storms, but also lift Asian dust into the upper troposphere and transport it along the westerly jet. The HYSPLIT
25 model shows the lower layer air was descending during transport from 7 May to 10 May 2007, which is similar to what was observed from CALIPSO for the dust. The behavior of the upper and lower dust layers is consistent with results from Huang et al. (2008).

The magnitude of the vertical extinction for the higher layer decreases from 0.1 km^{-1} (averaged from the CALIPSO data) and 0.12 km^{-1} (averaged from the model) on May

Saharan and asian dust

L. Su and O. B. Toon

Title Page

Abstract

Introduction

Conclusions

References

Tables

Figures

◀

▶

◀

▶

Back

Close

Full Screen / Esc

Printer-friendly Version

Interactive Discussion



Saharan and asian dust

L. Su and O. B. Toon

Title Page

Abstract

Introduction

Conclusions

References

Tables

Figures

◀

▶

◀

▶

Back

Close

Full Screen / Esc

Printer-friendly Version

Interactive Discussion



07 to 0.04 km^{-1} (averaged from the CALIPSO data) and 0.05 km^{-1} (averaged from the model) on 10 May 2007. There is a larger magnitude change for the extinction in the lower dust layer, which changes from 0.135 km^{-1} (averaged from the CALIPSO data) and 0.15 km^{-1} (averaged from the model) on 7 May to 0 (averaged from the CALIPSO data) and 0.05 km^{-1} (averaged from the model) on 9 May 2007.

In conclusion we find the vertical distributions of Asian and African dust are different. African dust is in a deep layer, the SAL, which descends at about 6 mm s^{-1} as it crosses the Atlantic. Asian dust does not form a deep layer, but is split by vertical wind shear into two layers in the case studied. Unlike African dust, the top layer shows no evidence of descent during transport.

3.3 Dust size distribution

The dust size distribution can be important for optical properties such as the wavelength dependence of the optical depth, and the single scattering albedo. Small particles (0.1 to $1.0 \mu\text{m}$ diameter) have larger scattering and absorbing cross sections per unit mass than large particles (Seinfeld and Pandis, 1998). We would like to know if Saharan and Asian dust particles have similar or different size distributions.

In order to interpret the size distributions we track layers of dust to AERONET sites. Figure 12 shows the 532-nm volume depolarization ratio from Saharan dust (around 15.02° N , 6.90° W) measured by CALIPSO. The dust fills the SAL from the ground to about 6 km altitude. There are cirrus clouds around 10° N , 8° W at 11 to 14 km altitudes that are distinguished from dust by their height and the fact that the lidar beam is almost totally attenuated beneath the cirrus. The volume depolarization ratio is computed from the total attenuated backscatter in the CALIPSO version 1 data products following Cairo et al. (1999) and Liu et al. (2008):

$$\delta(r) = \frac{\beta_{532,m,\perp}(r) + \beta_{532,p,\perp}(r)}{\beta_{532,m,\parallel}(r) + \beta_{532,p,\parallel}(r)} \quad (2)$$

Where $\beta_{532,m,\perp}(r)$ and $\beta_{532,p,\perp}(r)$ are the components of the backscatter signal po-

Saharan and asian dust

L. Su and O. B. Toon

Title Page

Abstract

Introduction

Conclusions

References

Tables

Figures

◀

▶

◀

▶

Back

Close

Full Screen / Esc

Printer-friendly Version

Interactive Discussion



larized perpendicular to the polarization plane of the linearly polarized laser pulse due to the molecular scattering and particulate scattering at range r and at the laser wavelength 532 nm, respectively. $\beta_{532,m,\parallel}(r)$ and $\beta_{532,p,\parallel}(r)$ are the components of the backscatter signal polarized parallel to the polarization plane of the linearly polarized laser pulse due to the molecular scattering and particulate scattering at range r and the laser wavelength 532nm, respectively. The values of the volume depolarization ratio of dust aerosols are usually between 0.06 to 0.3, whereas the ratio is below 0.06 (close to zero) for other aerosol types (Liu et al., 2008). The relatively high values of the dust depolarization ratios are due to the nonsphericity and large size of dust particles.

Figure 13 shows the 2-day back trajectories initialized on 21 July 2007 produced by HYSPLIT. The dust plumes originated over the Saharan Desert on 21 July 2007 and then arrived at Dakar (14.39° N, 16.95° W) on 22 July 2007. We chose to terminate the trajectories at Dakar because there is an AERONET site there.

Figure 14 shows the dust depolarization profile for Asian dust on 23 May 2007. Dust extends to about 8 km over the Gobi Deserts (between 45.0254° N, 109.356° E and 40.0556° N, 107.684° E) on 23 May 2007, but does not make a continuous layer to the surface. Figure 15 shows the 2-day back trajectories initialized on 23 May 2007 produced by HYSPLIT. The dust plumes originated at the Gobi Desert on 23 May 2007 and then reached Xianghe (39.75° N, 116.96° E) on 24 May 2007. We chose to terminate the trajectories at Xianghe because there is an AERONET site there as.

We compare the dust size distributions between Saharan and Asian dust during dust outbreaks. Considering the availability of AERONET observations, we choose Dakar on 22 July 2007 and Xianghe on 24 May 2007, which are close to dust sources, to represent Saharan and Asian dust, respectively.

Figures 16 and 17 present the modeled volume size distribution of Saharan dust at Dakar and the modeled volume size distribution of Asian dust at Xianghe, respectively. The model simulations are compared to AERONET measurements in each figure. The size distribution of Asian dust (Fig. 17) shows two volume modes, one near 0.5 μm and one near 2 μm radius. The Saharan distribution is unimodal with a peak slightly

Saharan and asian dust

L. Su and O. B. Toon

Title Page

Abstract

Introduction

Conclusions

References

Tables

Figures

◀

▶

◀

▶

Back

Close

Full Screen / Esc

Printer-friendly Version

Interactive Discussion



smaller than $2\ \mu\text{m}$. It is interesting that the model reproduces both of these distributions even though it uses identical dust source functions in each case. These volume mode radii have been verified by previous field campaigns both in Asia and in Sahara. McNaughton et al. (2009) indicated that the mode volume radius of the Asian dust is around $2\ \mu\text{m}$ radius based on the analysis from in-situ sampling of tropospheric aerosol during spring of 2006 in Phase B of the Intercontinental Chemical Transport Experiment (INTEX-B). Nowottnick et al. (2010) also found that the mode volume radius of Saharan dust is around 1 micron radius based on sampling during the African Monsoon Multi-disciplinary Analyses field campaign (August–September 2006). It should be noted that there are fine mode particles (such as nitrate, sulfate, and black carbon) in the AERONET size distribution data in Figs. 16 and 17 (around $0.1\ \mu\text{m}$ mode), but such particles have not been included in our model.

We suggest that the reason for the different numbers of size modes and the different mode radius values between African and Asian dust is related to the vertical ascent of the dust in the atmosphere. Figures 13 and 15 show that the air is sinking over the Sahara during transport at a rate of about $0.6\ \text{cm/s}$, but the air is rising over Asia at about $4\ \text{cm/s}$. Su and Toon (2008) illustrate the particle fall velocities, which show that a $4\ \text{cm/s}$ wind will suspend particles as large as $8\ \mu\text{m}$ radius.

We conclude that the particle size distributions in Saharan and Asian dust advected away from the sources likely differ, but these differences can be modeled using the same set of dust lifting functions. The differences are not related to surface mineralogy or lifting rates, but rather to different vertical velocities during transport.

3.4 Single scattering albedo

Figure 18 compares of the single scattering albedo between the model simulations and the AERONET retrievals both for Asian (Gobi) Desert (Dalanzadgad ($43.3^\circ\ \text{N}$, $104.3^\circ\ \text{E}$)) in April 2006 and the Sahara Desert (Tamanrasset_TMP ($22.5^\circ\ \text{N}$, $5.3^\circ\ \text{E}$)) in July 2006. We choose these two locations and time periods because they are close to the dust sources (while Dakar and Xianghe which we analyzed for size distributions

are downwind of dust sources), which minimize potential effects from air pollution, and also have cloud-screened and quality-assured AERONET data.

For the model, we assume the real part of the complex refractive index (assumed to be 1.55) is independent of wavelength both for Asian dust and Saharan dust based on the AERONET retrievals (Dubovik et al., 2000; Lyamani et al., 2005) and previous studies (Patterson et al., 1977; Diaz et al., 2000; Liu et al., 2002). We use data on the imaginary part of the refractive index from AERONET site measurements at the dust source regions that should be dominated by relative pure mineral dust particles. In downwind regions other pollutants such as nitrate, sulfate, and black carbon may alter the single scattering albedo. The imaginary part of the dust refractive index is constrained by the averaged AERONET value in April of 2006 at Dalanzadgad (0.0027, 0.0022, 0.0017, 0.0013 with increasing wavelength at 440 nm, 670 nm, 870 nm, and 1020 nm, respectively) for Asian dust and in July of 2006 at Tamanrasset_TMP (0.0036, 0.0031, 0.0026, 0.0020 with increasing wavelength at 440 nm, 670 nm, 870 nm, and 1020 nm, respectively) for Saharan dust. Figure 18 shows that the averaged single scattering albedo is larger for Asian dust than the Saharan dust. This is consistent with previous work suggesting that the dust transported from Asia to the Pacific may not absorb as much light as the dust from the Sahara Desert (Sokolik and Toon, 1999). The Asian dust has a smaller imaginary refractive index than Saharan dust, which is main reason the Asian dust has a higher single scattering albedo near the source. The single scattering albedos may depend on size as well, particularly as the size distributions are modified downwind of the sources as discussed previously.

4 Summary and conclusions

Using our model we find that the yearly annual dust flux from Africa is about 4 times greater than that from Asia. In general, it is observed that the dust optical depth is higher over the Atlantic than over the Pacific at similar downwind distances from the two dust sources. The monthly-averaged optical depth is 0.382 and 0.339 over the

Saharan and asian dust

L. Su and O. B. Toon

Title Page

Abstract

Introduction

Conclusions

References

Tables

Figures

◀

▶

◀

▶

Back

Close

Full Screen / Esc

Printer-friendly Version

Interactive Discussion



Pacific at Osaka in May 2007 for AERONET data and model simulation, respectively. However, the monthly-averaged optical depth is 0.613 and 0.579 over Atlantic at Capo Verde in July 2007 for AERONET data and model simulation, respectively. Hence even during peak months for dust lifting in Asia, smaller dust optical depths occur than during peak months in Africa.

The annual dust flux near the dust source is about 1446 Tg/year across 10° E (10° S–40° N, 10° E) and 355 Tg/year across 105° E (25° N–55° N, 105° E) for Sahara and Asia in 2007, respectively. Saharan deserts are largely south of 30° N, while Asian ones are primarily north of 30° N. This leads them to experience different meteorological regimes. Saharan dust lifting occurs all year long, primarily due to subtropical weather systems. The Saharan dust transport into the Caribbean is controlled primarily by a semi-permanent high, the Azores High. The annual dust cycle of the African dust sources can be triggered and modulated by synoptic systems, such as African easterly waves, in the Atlantic region. The dust outbreaks usually occur within the ridge region of passing easterly waves with a period of 5–7 days. In contrast, 45% of Asian dust was lifted in spring during the modeled year of 2007 when mid-latitude frontal systems lead to high winds. The seasonal variation of dust outbreaks in Asia is associated with the seasonal modulation of the wind speed. Strong winds occur most frequently in spring in Asia due to the activity of the mid-latitude frontal systems. The mid-latitude frontal cyclones associated with intense cold fronts from Mongolia to northeastern China not only generate dust storms, but can also lift Asian dust into the westerly jet in the upper troposphere.

Rainfall is more abundant over Asia during the dust lifting events than over the Sahara, leading to greater local dust removal than over the Sahara. However, wet removal is a small fraction of the total removal of dust, and removal processes do not account for the difference in annual dust flux between the Sahara and Asia. Instead, the Sahara simply has about three times as much area with dust lifting as Asia because Asia has smaller deserts and also more vegetation and snow cover, which suppresses dust lifting.

Saharan and asian dust

L. Su and O. B. Toon

Title Page

Abstract

Introduction

Conclusions

References

Tables

Figures

◀

▶

◀

▶

Back

Close

Full Screen / Esc

Printer-friendly Version

Interactive Discussion



Saharan and asian dust

L. Su and O. B. Toon

[Title Page](#)[Abstract](#)[Introduction](#)[Conclusions](#)[References](#)[Tables](#)[Figures](#)[I◀](#)[▶I](#)[◀](#)[▶](#)[Back](#)[Close](#)[Full Screen / Esc](#)[Printer-friendly Version](#)[Interactive Discussion](#)

During the major lifting season the power averaged winds over Africa and Asia are similar. However in other seasons Africa has stronger winds than does Asia, which further contributes to more dust lifting over Africa. The power-averaged wind contributes about a factor of 1.7 to the differences of the total dust fluxes between the two sources averaged over the year.

The vertical distribution of Asian and African dust also differs in the cases we considered. The Saharan dust is primarily located in a deep layer, the SAL. The top of the layer descends during transport, which we conclude is mainly due to descending air in the Azores High. There are two noticeable layers of Asian dust during transport in May. One layer stays well above boundary layer, and does not descend with time. The other layer is in a shallow near surface boundary layer and descends with time. The transport of Asian dust is dominated by the westerlies at high altitudes, while it is controlled by regional weather systems and topography at lower altitudes. Sedimentation does not seem to play a significant role in the descent of long lasting layers. Horizontal wind shear can also play a role in the vertical extent of dust layers by moving dust horizontally.

The size distribution of Asian dust (at Xianghe) is bi-modal while that of Saharan dust (at Dakar) is uni-modal. The volume size distribution of Asian dust peaks around 2 microns, whereas it peaks around 1 micron for Saharan dust. Both model simulations and the AERONET retrievals show similar patterns. We suggest these differences originate from the vertical winds that occur during transport. For the case we studied, winds over Africa were descending, while those over Asia were ascending. The ascending winds were strong enough to loft dust particles as large as about 8 μm .

We assume the real part of the complex refractive index is independent of wavelength (1.55) both for Asian dust and Saharan dust based on the AERONET retrievals and previous studies. We use data on the imaginary part of the refractive index from AERONET site measurements near the dust source regions. We find that the average single scattering albedo is larger for Asian dust than the Saharan dust. This is consistent with the refractive indices inferred by AERONET for the two dust sources, and

with a previous study that the dust transported from Asia to the Pacific may not absorb as much light as the dust from the Sahara. As the size distribution evolves downwind of the sources due to the vertical winds experienced during transport, and as pollutants are added to the dust, the single scattering albedos will evolve.

5 *Acknowledgements.* Lin Su was partly supported by the NASA Earth and Space Science Fellowship Program-Grant 10-Earth10R-10. NSF grant ATM-0856007 also supported this work as did the CALIPSO science team under NN07AR13G. The CALIPSO program data were obtained from the NASA Langley Research Center Atmospheric Science Data Center. We thank AERONET staff for establishing and maintaining the sites used in this investigation of
10 the AERONET data. We also acknowledge Z. Liu, P. R. Colarco, A. Gettelman, and X. Liu for helpful discussion. We gratefully thank the reviewers for their valuable time and helpful suggestions.

References

- 15 Ackerman, A. S., Hobbs, P. V., and Toon, O. B.: A model for particle microphysics, turbulent mixing, and radiative transfer in the stratocumulus-topped marine boundary layer and comparisons with measurements, *J. Atmos. Sci.*, 52, 1204–1236, 1995.
- Arellano Jr., A. F., Raeder, K., Anderson, J. L., Hess, P. G., Emmons, L. K., Edwards, D. P., Pfister, G. G., Campos, T. L., and Sachse, G. W.: Evaluating model performance of an ensemble-based chemical data assimilation system during INTEX-B field mission, *Atmos. Chem. Phys.*, 7, 5695–5710, doi:10.5194/acp-7-5695-2007, 2007.
- 20 Barth, M. C., Rasch, P. J., Kiehl, J. T., Benkovitz, C. M., and Schwartz, S. E.: Sulfur chemistry in the National Center for Atmospheric Research Community Climate Model: Description, evaluation, features, and sensitivity to aqueous chemistry, *J. Geophys. Res.*, 105, 1387–1415, 2000.
- 25 Betzer, P. R., Carder, K. L., Duce, R. A., Merrill, J. T., and Tindale, N. W.: Long-range transport of giant mineral aerosol particles, *Nature*, 336, 568–571, 1998.
- Cairo F., Donfrancesco, G., Adriani, A., Pulvirenti, L., and Fierli F.: Comparison of Various Linear Depolarization Parameters Measured by Lidar, *Appl. Opt.*, 38, 4425–4432, 1999.
- Carmichael, G. R., Tang, Y., Kurata, G., Uno. I., Streets, D., Woo, J., Huang, H., Yienger, J.,

Saharan and asian dust

L. Su and O. B. Toon

Title Page

Abstract

Introduction

Conclusions

References

Tables

Figures

◀

▶

◀

▶

Back

Close

Full Screen / Esc

Printer-friendly Version

Interactive Discussion



Saharan and asian dust

L. Su and O. B. Toon

Title Page

Abstract

Introduction

Conclusions

References

Tables

Figures

◀

▶

◀

▶

Back

Close

Full Screen / Esc

Printer-friendly Version

Interactive Discussion



Lefer, B., Shetter, R., Blake, D., Atlas, E., Fried, A., Apel, E., Eisele, F., Cantrell, C., Avery, M., Barrick, J., Sachse, G., Brune, W., Sandholm, S., Kondo, Y., Singh, H., Talbot, R., Bandy, A., Thornton, D., Clarke, A., and Heikes, B.: Regional-scale chemical transport modeling in support of intensive field experiments: Overview and analysis of the TRACE-P observations, *J. Geophys. Res.*, 108(D21), 8823, doi:10.1029/2002JD003117, 2003.

Chin, M., Ginoux, P., Lucchesi, R., Huebert, B., Weber, E., Anderson, T., Masonis, S., Blomquist, B., Bandy, A., and Thornton, D.: A global aerosol model forecast for the ACE-Asia field experiment, *J. Geophys. Res.*, 108(D23), 8654, doi:10.1029/2003JD003642, 2003.

Chin, M., Chu, D. A., Levy, R., Remer, L. A., Kaufman, Y. J., Holben, B. N., Eck, T., and Ginoux, P.: Aerosol distribution in the Northern Hemisphere during ACE-Asia: Results from global model, satellite observations, and Sun photometer measurements, *J. Geophys. Res.*, 109, D23S90, doi:10.1029/2004JD004829, 2004.

Clarke, A. D., Collins, W. G., Rasch, P. J., Kapustin, V. N., Moore, K., Howell, S., and Fuelberg, H. E.: Dust and pollution transport on global scales: Aerosol measurements and model predictions, *J. Geophys. Res.*, 106, 32,555–32,569, 2001.

Colarco, P. R., Toon, O. B., Torres, O., and Rasch, P. J.: Determining the UV imaginary index of refraction of Saharan dust particles from Total Ozone Mapping Spectrometer data using a three-dimensional model of dust transport, *J. Geophys. Res.*, 107 (D16), 4312, doi:10.1029/2001JD000903, 2002.

Colarco, P. R., Toon, O. B., Holben, B. N.: Saharan dust transport to the Caribbean during PRIDE: 1. Influence of dust sources and removal mechanisms on the timing and magnitude of downwind aerosol optical depth events from simulations of in situ and remote sensing observations, *J. Geophys. Res.*, 108(D19), 8589, doi:10.1029/2002JD002658, 2003a.

Colarco, P. R., Toon, O. B., Reid, J. S., Livingston, J. M., Russell, P. B., Redemann, J., Schmid, B., Maring, H. B., Savoie, D., Welton, E. J., Campbell, J. R., Holben, B. N., and Levy, R.: Saharan dust transport to the Caribbean during PRIDE: 2. Transport, vertical profiles, and deposition in simulations of in situ and remote sensing observations, *J. Geophys. Res.*, 108(D19), 8590, doi:10.1029/2002JD002659, 2003b.

Collins, W. D., Rasch, P. J., Boville, B. A., Hack, J. J., McCaa, J. R., Williamson, D. L., Kiehl, L. T., Briegleb, B., Bitz, C., Lin, S., Zhang, M., and Dai, Y. 9. Page 27, line 7: Dubovik, O., Smirnov, A., Holben, B. N., King, M. D., Kaufman, Y. J., and Slutsker, I.: Description of the NCAR Community Atmosphere Model (CAM3.0), Technical Report NCAR/TN-464+STR, National Center for Atmospheric Research, Boulder, Colorado, 210 pp., 2004.

Saharan and asian dust

L. Su and O. B. Toon

[Title Page](#)[Abstract](#)[Introduction](#)[Conclusions](#)[References](#)[Tables](#)[Figures](#)[◀](#)[▶](#)[◀](#)[▶](#)[Back](#)[Close](#)[Full Screen / Esc](#)[Printer-friendly Version](#)[Interactive Discussion](#)

- Cuesta J., Marsham J. H., and Parker D. J.: Flamant C, Dynamical mechanisms controlling the vertical redistribution of dust and the thermodynamic structure of the West Saharan atmospheric boundary layer during summer, *Atmos. Sci. Lett.*, 10, 34–42, 2009.
- Díaz, J. P., Exposito, F. J., Torres, C. J., Carreño, V., and Redondas, A.: Simulation of mineral dust effects on UV-radiation levels, *J. Geophys. Res.*, 105, 4979–4991, 2000.
- Doherty, O. M., Riemer, N., and Hameed, S.: Saharan mineral dust transport into the Caribbean: Observed atmospheric controls and trends, *J. Geophys. Res.*, 113, D07211, doi:10.1029/2007JD009171, 2008.
- Draxler, R. R. and Rolph, G. D.: HYSPLIT (Hybrid Single-Particle Lagrangian Integrated Trajectory) model, Air Resour. Lab., NOAA, Silver Spring, Md. (available at: <http://www.arl.noaa.gov/ready/hysplit4.html>), 2003.
- Dubovik, O., Smirnov, A., Holben, B. N., King, M. D., Kaufman, Y. J., and Slutsker, I.: Accuracy assessments of aerosol optical properties retrieved from AERONET sun and sky radiance measurements, *J. Geophys. Res.*, 105, 9791–9806, 2000.
- Duce, R.: The atmospheric input of trace species to the world ocean, *Global Biogeochem. Cycle*, 5, 193–259, 1991.
- Duce, R. A., Unni, C. K., Ray, B. J., Prospero, J. M., and Merrill, J. T.: Long-range atmospheric transport of soil dust from Asia to the tropical North Pacific: temporal variability, *Science*, 209, 1522–1524, 1980.
- Dunion, J. P. and Velden, C. S.: The impact of Saharan air layer on Atlantic tropical cyclone activity, *Bull. Am. Meteorol. Soc.*, 85, 353–365, doi:10.1175/BAMS-85-3-353, 2004.
- Nowottnick, E., Colarco, P., Ferrare, R., Chen, G., Ismail, S., Anderson, B., and Browell, E.: Online simulations of mineral dust aerosol distributions: Comparisons to NAMMA observations and sensitivity to dust emission parameterization, *J. Geophys. Res.*, 115, D03202, doi:10.1029/2009JD012692, 2010.
- Eguchi, K., Uno, I., Yumimoto, K., Takemura, T., Shimizu, A., Sugimoto, N., and Liu, Z.: Transpacific dust transport: integrated analysis of NASA/CALIPSO and a global aerosol transport model, *Atmos. Chem. Phys.*, 9, 3137–3145, doi:10.5194/acp-9-3137-2009, 2009.
- Fernald, F. G.: Analysis of atmospheric lidar observations: some comments, *Appl. Opt.*, 23, 652–653, 1984.
- Fernald F. G., Herman B. M., Reagan J. A.: Determination of aerosol height distributions by lidar, *Journal of Atmospheric Meteorology*, 11, 482–489, 1972.
- Gillette, D. A., and Passi, R.: Modeling dust emission caused by wind erosion, *J. Geophys.*

Saharan and asian dust

L. Su and O. B. Toon

Title Page

Abstract

Introduction

Conclusions

References

Tables

Figures

◀

▶

◀

▶

Back

Close

Full Screen / Esc

Printer-friendly Version

Interactive Discussion



Res., 93, 14233–14242, 1988.

Gomes, L., Bergametti, G., Coud'e-Gaussen, G., and Rognon, P.: Submicron desert dusts: A sandblasting process, *J. Geophys. Res.*, 95, 13927–13935, 1990.

Gong, S. L., Zhang, X. Y., Zhao, T. L., McKendry, I. G., Jaffe, D. A., and Lu, N. M.: Characterization of soil dust aerosol in China and its transport and distribution during 2001 ACE-Asia: 2. Model simulation and validation, *J. Geophys. Res.*, 108(D9), 4262, doi:10.1029/2002JD002633, 2003.

Generoso, S., Bey, I., Labonne, M., and Bréon, F. M.: Aerosol vertical distribution in dust outflow over the Atlantic: Comparisons between GEOS-Chem and Cloud-Aerosol Lidar and Infrared Pathfinder Satellite Observation (CALIPSO), *J. Geophys. Res.*, 113, D24209, doi:10.1029/2008JD010154, 2008.

Ginoux, P., Chin, M., Tegen, I., Prospero, J. M., Holben, B., Dubovik, O., and Lin, S. J.: Sources and distributions of dust aerosols simulated with the GOCART model, *J. Geophys. Res.*, 106, 20,255–20,273, 2001.

Grousset F. E., Ginoux, P., Bory, A., and Biscaye, P. E.: Case study of a Chinese dust pume reaching the French Alps, *Geophys. Res. Lett.*, 30, 1277, doi:10.029/2002/g1016833, 2003.

Haywood, J. M., Allan, R. P., Culverwell, I., Slingo, A., Milton, S. F., Edwards, J. M., and Clerbaux, N.: Can desert dust explain the outgoing longwave radition anomaly over the Sahara during July 2003, *J. Geophys. Res.-Atmos.*, 110, D05105, 2005.

Haywood, J. M., Pelon, J., Formenti, P., Bharmal, N., Brooks, M., Capes, G., Chazette, P., Chou. C., Christopher, S., Coe, H., Cuesta, J., Derimian, Y., Desboeufs, K., Greed, G., Harrison, M., Heese, B., Highwood, E. J., Johnson, B., Mallet, M., Marticorena, B., Marsham, J., Milton, S., Myhre, G., Osborne, S. R., Parker, D. J., Rajot, J. -L., Schulz, M., Slingo, A., Tanre, D., and Tulet, P.: Overview of the Dust and Biomass-burning Experiment and African Monsoon Multidisciplinary Analysis Special Observing Period-0, *J. Geophys. Res.*, 113, D00C17, doi:10.1029/2008JD010077, 2008.

Heese, B. and Wiegner, M.: Vertical aerosol profiles from Raman polarization lidar observations during the dry season AMMA field campaign, *J. Geophys. Res.*, 113, D00C11, doi:10.1029/2007JD009487, 2008.

Heintzenberg, J.: The SAMUM-1 experiment over Southern Morocco: overview and introduction, *Tellus*, 61(1), 2–11, doi:10.1111/j.1600-0889.2008.00403.x, 2008.

Holben, B. N., Eck, T. F., Slutsker, I., Tanreacut;, D., Buis, J. P., Setzer, A., Vermote, E. F., Reagan, J. A., Kaufman, Y. J., Nakajima, T., Lavenu, F., Jankowiak, I., and Smirnov, A.:

Saharan and asian dust

L. Su and O. B. Toon

Title Page

Abstract

Introduction

Conclusions

References

Tables

Figures

◀

▶

◀

▶

Back

Close

Full Screen / Esc

Printer-friendly Version

Interactive Discussion



AERONET-A federated instrument network and data archive for aerosol characterization, *Remote Sens. Environ.*, 66, 1–16, 1998.

Huang, J., Minnis, P., Yi, Y., Tang, Q., Wang, X., Hu, Y., Liu, Z., Ayers, K., Treppe, C., and Winker, D.: Summer dust aerosols detected from CALIPSO over the Tibetan Plateau, *Geophys. Res. Lett.*, 34, L18805, doi:10.1029/2007GL029938, 2007.

Huang, J., Minnis, P., Chen, B., Huang, Z., Liu, Z., Zhao, Q., Yi, Y., and Ayers, J. K.: Long-range transport and vertical structure of Asian dust from CALIPSO and surface measurements during PACDEX, *J. Geophys. Res.*, 113, D23212, doi:10.1029/2008JD010620, 2008.

Huang, J., Fu, Q., Su, J., Tang, Q., Minnis, P., Hu, Y., Yi, Y., and Zhao, Q.: Taklimakan dust aerosol radiative heating derived from CALIPSO observations using the Fu-Liou radiation model with CERES constraints, *Atmos. Chem. Phys.*, 9, 4011–4021, doi:10.5194/acp-9-4011-2009, 2009.

Huebert, B. J., Bates, T., Russell, P. B., Shi, G., Kim, Y., Kawamura, K., Carmichael, G., and Nakajima, T.: An overview of ACE-Asia: Strategies for quantifying the relationships between Asian aerosols and their climatic impacts, *J. Geophys. Res.*, 108(D23), 8633, doi:10.1029/2003JD003550, 2003.

Husar, R. B., Tratt, D. M., Schichtel, B. A., Falke, S. R., Li, F., Jaffe, D., Gasso, S., Gill, T., Laulainen, N. S., Lu, F., Reheis, M. C., Chun, Y., Westphal, D., Holben, B. N., Gueymard, C., McKendry, I., Kuring, N., Feldman, G. C., McClain, C., Frouin, R. J., Merrill, J., DuBois, D., Vignola, F., Murayama, T., Nickovic, S., Wilson, W. E., Sassen, K., Sugimoto, N., and Malm, W. C.: Asian dust events of April 1998, *J. Geophys. Res.*, 106, 18,317–18,330, 2001.

IPCC, *Climate Change 2007: The Physical Science Basis*, Contribution of Working Group 1 to the Fourth Assessment Report of the Intergovernmental Panel On Climate Change, edited by: Solomon, S., Qin, D., Manning, M., Chen, Z., Marquis, M., Averyt, K. B., Tignor, M., and Miller, H. L., Cambridge University Press, Cambridge, United Kingdom and New York, NY, USA, 2007.

Jacob, D. J., Crawford, J. H., Kleb, M. M., Connors, V. S., Bendura, R. J., Raper, J. L., Sachse, G. W., Gille, J. C., Emmons, L., and Heald, C. L.: Transport and Chemical Evolution Over the Pacific (TRACE-P) aircraft mission: Design, execution, and first results, *J. Geophys. Res.*, 108(D20), 9000, doi:10.1029/2002JD003276, 2003.

Jensen, E. J., Toon, O. B., Westphal, D. L., Kinne, S., and Heymsfield, A. J.: Microphysical modeling of cirrus: 1. Comparison with 1986 FIRE IFO measurements, *J. Geophys. Res.*, 99, 10,421–10,442, 1994.

- Jones, C., Mahowald, N., and Luo, C.: The role of easterly waves on African desert dust transport, *J. Clim.*, 16(22), 3617–3628, 2003.
- Kandler, K., Schutz, L., Deutscher, C., Ebert, M., Hofmann, H., Jackel, S., Jaenicke, R., Knipertz, P., Lieke, K., Massling, A., Petzold, A., Schladitz, A., Weinzierl, B., Wiedensohler, A., Zorn, S., Weinbruch, S. 16. Page 29, line 28: Karyampudi, V. M., Palm, S. P., Reagen, J. A., Fang, H., Grant, W. B., Hoff, R. M., Moulin, C., Pierce, H. F., Torres, O., Browell, E. V., and Melfi, S. H.: Size distribution, mass concentration, chemical and mineralogical composition and derived optical parameters of the boundary layer aerosol at Tinfou, Morocco, during SAMUM 2006, 32–50, doi:10.1111/j.1600-0889.2008.00385.x, 2008.
- Karyampudi, V. M., Palm, S. P., Reagen, J. A., Fang, H., Grant, W. B., Hoff, R. M., Moulin, C., Pierce, H. F., Torres, O., Browell, E. V., and Melfi, S. H.: Validation of the Saharan dust plume conceptual model using lidar, Meteosat, and ECMWF data, *Bull. Am. Meteorol. Soc.*, 80, 1045–1075, 1999.
- Kaufman, Y. J. and Fraser, R. S.: The effect of smoke particles on cloud and climate forcing, *Science*, 277, 1636–1639, 1997.
- Kaufman, Y. J., Tanre, D., Dubovik, O., Karnieli, A., and Remer, L. A.: Absorption of sunlight by dust as Inferred from satellite and ground-based remote sensing. *Geophys. Res. Lett.*, 28, 1479–1483, 2001.
- Laurent, B., Martcorena, B., Bergametti, G., and Mei, F.: Modeling mineral dust emissions from Chinese and Mongolian deserts, *Global. Planet. Change.*, 52, 121–141, 2006.
- Lee, E.-H. and Sohn, B.-J.: Examining the impact of wind and surface vegetation on the Asian dust occurrence over three classified source regions, *J. Geophys. Res.*, 114, D06205, doi:10.1029/2008JD010687, 2009.
- Levin, Z., Ganor, E., and Gladstein, V.: The effects of desert particles coated with sulfate on rain formation in the eastern Mediterranean, *J. Appl. Meteorol.*, 35, 1511–1523, 1996.
- Lin, S. J. and Rood, R. B.: Multidimensional flux-form semi-Lagrangian transport schemes, *Mon. Wea. Rev.*, 124, 2046–2070, 1996.
- Liu, D., Wang, Z., Liu, Z., Winker, D., and Trepte, C.: A height resolved global view of dust aerosols from the first year CALIPSO lidar measurements, *J. Geophys. Res.*, 113, D16214, doi:10.1029/2007JD009776, 2008.
- Liu, X., Penner, J. E., and Herzog, M.: Global modeling of aerosol dynamics: Model description, evaluation, and interactions between sulfate and nonsulfate aerosols, *J. Geophys. Res.*, 110, D18206, doi:10.1029/2004JD005674, 2005.

Saharan and asian dust

L. Su and O. B. Toon

Title Page

Abstract

Introduction

Conclusions

References

Tables

Figures

◀

▶

◀

▶

Back

Close

Full Screen / Esc

Printer-friendly Version

Interactive Discussion



Saharan and asian dust

L. Su and O. B. Toon

[Title Page](#)[Abstract](#)[Introduction](#)[Conclusions](#)[References](#)[Tables](#)[Figures](#)[◀](#)[▶](#)[◀](#)[▶](#)[Back](#)[Close](#)[Full Screen / Esc](#)[Printer-friendly Version](#)[Interactive Discussion](#)

- Liu, Z., Sugimoto, N., and Murayama, T.: Extinction-to-backscatter ratio of Asian dust observed by high-spectral-resolution lidar and Raman lidar, *Appl. Opt.*, 41, 2760–2767, 2002.
- Liu, Z., Hunt, W., Vaughan, M., Hostetler, C., McGill, M., Powell, K., Winker, D., and Hu, Y.: Estimating random errors due to shot noise in backscatter lidar observations, *Appl. Opt.*, 45, 4437–4447, 2006.
- Liu, Z., Liu, D., Huang, J., Vaughan, M., Uno, I., Sugimoto, N., Kittaka, C., Trepte, C., Wang, Z., Hostetler, C., and Winker, D.: Airborne dust distributions over the Tibetan Plateau and surrounding areas derived from the first year of CALIPSO lidar observations, *Atmos. Chem. Phys.*, 8, 5045–5060, doi:10.5194/acp-8-5045-2008, 2008a.
- Liu, Z., Omar, A., Vaughan, M., Hair, J., Kittaka, C., Hu, Y., Powell, K., Trepte, C., Winker, D., Hostetler, C., Ferrare, R., and Pierce, R.: CALIPSO lidar observations of the optical properties of Saharan dust: A case study of long-range transport, *J. Geophys. Res.*, 113, D07207, doi:10.1029/2007JD008878, 2008b.
- Lyamani, H., Olmo, F. J., and Alados-Arboledas, L.: Saharan dust outbreak over southeastern Spain as detected by sun photometer, *Atmos. Environ.*, 39(38), 7276–7284, 2005.
- Mahowald, N., Kohfeld, K., Hansson, M., Balkanski, Y., Harrison, S. P., Printice, I. C., Schulz, M., Rodhe, H.: Dust sources and deposition during the last glacial maximum and current climate: a comparison of model results with paleodata from ice cores and marine sediments, *J. Geophys. Res.* 104, 15895–15916, 1999.
- Mahowald, N., Yoshioka, M., Collins, W., Conley, A., Fillmore, D., Coleman, D.: Climate response and radiative forcing from mineral aerosols during the glacial maximum, pre-industrial, current and doubled-carbon dioxide climates, *GRL*, 33, L20705, doi:10.1029/2006GL026126, 2006.
- Maring, H., Savoie, D. L., Izaguirre, M. A., and Custals, L.: Vertical distributions of dust and sea salt over Puerto Rico during PRIDE measured from a light aircraft, *J. Geophys.*, 108, doi:10.1029/2002JD002544, 11 pp., 2003.
- Marshall, J. H., Parker, D. J., Grams, C. M., Johnson, B. T., Grey, W. M. F., and Ross, A. N.: Observations of mesoscale and boundary-layer scale circulations affecting dust transport and uplift over the Sahara, *Atmos. Chem. Phys.*, 8, 6979–6993, doi:10.5194/acp-8-6979-2008, 2008.
- Marticorena, B., Bergametti, G., Aumont, B., Callot, Y., N'Doum'e, C., and Legrand, M.: Modeling the atmospheric dust cycle: 2. Simulation of Saharan dust sources, *J. Geophys. Res.*, 102, 4387–4404, doi:10.1029/96JD02964, 4387–4404, 1997.

Saharan and asian dust

L. Su and O. B. Toon

Title Page

Abstract

Introduction

Conclusions

References

Tables

Figures

◀

▶

◀

▶

Back

Close

Full Screen / Esc

Printer-friendly Version

Interactive Discussion



- Martin, J. H.: Testing the iron hypothesis in ecosystem of the equatorial Pacific Ocean, *Nature*, 371, 123–129, 1994.
- McKendry, I. G., Macdonald, A. M., Leaitch, W. R., van Donkelaar, A., Zhang, Q., Duck, T., and Martin, R. V.: Trans-Pacific dust events observed at Whistler, British Columbia during INTEX-B, *Atmos. Chem. Phys.*, 8, 6297–6307, doi:10.5194/acp-8-6297-2008, 2008.
- McNaughton, C. S., Clarke, A. D., Kapustin, V., Shinozuka, Y., Howell, S. G., Anderson, B. E., Winstead, E., Dibb, J., Scheuer, E., Cohen, R. C., Wooldridge, P., Perring, A., Huey, L. G., Kim, S., Jimenez, J. L., Dunlea, E. J., DeCarlo, P. F., Wennberg, P. O., Crounse, J. D., Weinheimer, A. J., and Flocke, F.: Observations of heterogeneous reactions between Asian pollution and mineral dust over the Eastern North Pacific during INTEX-B, *Atmos. Chem. Phys.*, 9, 8283–8308, doi:10.5194/acp-9-8283-2009, 2009.
- Müller, D., Heinold, B., Tesche, M., Tegen, I., Althausen, D., Arboledas, L. A., Amiridis, V., Amodeo, A., Ansmann, A., Balis, D., Comeron, A., D’Amico, G., Gerasopoulos, E., Guerrero-Rascado, J. L., Freudenthaler, V., Giannakaki, E., Heese, B., Iarlori, M., Knippertz, P., Mamouri, R. E., Mona, L., Papayannis, A., Pappalardo, G., Perrone, R.-M., Pisani, G., Rizi, V., Sicard, M., Spinelli, N., Tafuro, A., and Wiegner, M.: EARLINET observations of the 14–22-May long-range dust transport event during SAMUM 2006: validation of results from dust transport modeling, *Tellus*, 61B, 325–339, doi:10.1111/j.1600-0889.2008.00400.x, 2008.
- Patterson E. M., Gillette, D., and Stockton, B. H.: Complex index of refraction between 300 and 700 nm for Saharan aerosols, *J. Geophys. Res.*, 82, 3153–3160, 1997.
- Pfister, L., Selkirk, H. B., Starr, D. O., Rosenlof, K., and Newman, P. A.: A Meteorological Overview of the TC4 Mission, *J. Geophys. Res.*, 115, 24 pp., doi:10.1029/2009JD013316, 2010.
- Prospero, J.: The atmospheric transport of particles to the ocean, in *Particle Flux in the Ocean*, 18–152, John Wiley, New York, USA, 1996.
- Prospero, J.: Long-term measurements of the transport of African mineral dust to the south-eastern United States: Implications for regional air quality, *J. Geophys. Res.*, 104, 15,917–15,927, 1999.
- Prospero, J. M. and Carlson, T. N.: Vertical and areal distribution of Saharan dust over the western equatorial North Atlantic ocean, *J. Geophys. Res.*, 77 5255–65, 1972.
- Prospero, J. M. and Carlson, T. N.: Saharan air outbreaks over the tropical North Atlantic, *Pure Appl. Geophys.*, 119, 677–691, 1981.
- Prupacher, H. R. and Klett, J. D.: *Microphysics of Clouds and Precipitation*, Kluwer Academic

Saharan and asian dust

L. Su and O. B. Toon

Title Page

Abstract

Introduction

Conclusions

References

Tables

Figures

◀

▶

◀

▶

Back

Close

Full Screen / Esc

Printer-friendly Version

Interactive Discussion



Publishers, 954 pp., 1997.

Rajot, J. L., Formenti, P., Alfaro, S., Desboeufs, K., Chevaillier, S., Chatenet, B., Gaudichet, A., Journet, E., Marticorena, B., Triquet, S., Maman, A., Mouget, N., and Zakou, A.: AMMA dust experiment: An overview of measurements performed during the dry season special observation period (SOP0) at the Banizoumbou (Niger) supersite, *J. Geophys. Res.*, 113, D00C14, doi:10.1029/2008JD009906, 2008.

Ramanathan, V., Crutzen, P. J., Lelieveld, J., Mitra, A. P., Althausen, D., Anderson, J., Andreae, M. O., Cantrell, W., Cass, G. R., Chung, C. E., Clarke, A. D., Coakley, J. A., Collins, W. D., Conant, W. C., Dulac, F., Heintzenberg, J., Heyms?eld, A. J., Holben, B., Howell, S., Hudson, J., Jayaraman, A., Kiehl, J. T., Krishnamurti, T. N., Lubin, D., McFarquhar, G., Novakov, T., Ogren, J. A., Podgorny, I. A., Prather, K., Priestley, K., Prospero, J. M., Quinn, P. K., Rajeev, K., Rasch, P., Rupert, S., Sadourny, R., Satheesh, S. K., Shaw, G. E., Sheridan, P., and Valero, F. P. J.: The Indian Ocean Experiment: An integrated assessment of the climate forcing and effects of the great Indo-Asian haze, *J. Geophys. Res.*, 106(D22), 28,371–28,399, doi:10.1029/2001JD900133, 2001.

Rasch, P. J., Mahowald, N. M., and Eaton, B. E.: Representations of transport, convection, and the hydrologic cycle in chemical transport models: Implications for the modeling of short-lived and soluble species, *J. Geophys. Res.*, 102, 28,127–28,138, 1997.

Rasch, P. J., Collins, W. D., and Eaton, B. E.: Understanding the Indian Ocean Experiment (INDOX) aerosol distributions with an aerosol assimilation, *J. Geophys. Res.*, 106, 7337–7355, 2001.

Rea, D. K., Leinen, M., and Janecek, T. R.: Geologic approach to the long-term history of atmospheric circulation, *Science*, 227, 721–725, 1985.

Reid, J. S., Westphal, D. L., Livingston, J. M., Savoie, D. L., Maring, H. B., Jonsson, H. H., Eleuterio, D. P., Kinney, J. E., and Reid, E. A.: Dust vertical distribution in the Caribbean during the Puerto Rico Dust Experiment, *Geophys. Res. Lett.*, 29(7), 1151, doi:10.1029/2001GL014092, 2002.

Reid, J. S., Kinney, J. E., Westphal, D. L., Holben, B. N., Welton, E. J., Tsay, S., Eleuterio, D. P., Campbell, J. R., Christopher, S. A., Colarco, P. R., Jonsson, H. H., Livingston, J. M., Maring, H. B., Meier, M. L., Pilewskie, P., Prospero, J. M., Reid, E. A., Remer, L. A., Russell, P. B., Savoie, D. L., Smirnov, A., and Tanré, D.: Analysis of measurements of Saharan dust by airborne and ground-based remote sensing methods during the Puerto Rico Dust Experiment (PRIDE), *J. Geophys. Res.*, 108(D19), 8586, doi:10.1029/2002JD002493, 2003b.

Saharan and asian dust

L. Su and O. B. Toon

Title Page

Abstract

Introduction

Conclusions

References

Tables

Figures

◀

▶

◀

▶

Back

Close

Full Screen / Esc

Printer-friendly Version

Interactive Discussion



Sassen, K.: Lidar backscatter depolarization technique for cloud and aerosol research, in *Light Scattering by Nonspherical Particles: Theory, Measurements, and Geophysical Applications*, edited by: Mishchenko, M. L., Hovenier, J. W., and Travis, L. D., 393–416, Academic Press, San Diego, 2000.

5 Schulz, M., Balkanski, Y., Guelle, W., and Dulac, F.: Role of aerosol size distribution and Source location in a three dimensional simulation of a saharan dust episode tested against satellite derived optical thickness, *J. Geophys. Res.*, 103, 10579–10592, 1998.

Seinfeld, J. H. and Pandis, S. N.: *Atmospheric Chemistry and Physics: From Air Pollution to Climate Change*, John Wiley&Sons, New York, Chichester, Weinheim, Brisbane, Singapore, and Toronto, 1998.

10 Seinfeld, J. H., Carmichael, G. R., Arimoto, R., Conant, W. C., Brechtel, F. J., Bates, T. S., Cahill, T. A., Clarke, A. D., Doherty, S. J., Flatau, P. J., Huebert, B. J., Kim, J., Markowicz, K. M., Quinn, P. K., Russell, L. M., Russell, P. B., Shimizu, A., Shinzuka, Y., Song, C. H., Tang Y., Uno, I., Vogelmann, A. M., Weber, R. J., Woo, J., and Zhang, Y.: ACE-ASIA-Regional climatic and atmospheric chemical effects of Asian dust and pollution, *Bull. Am. Meteorol. Soc.*, 85(3), 367–380, doi:10.1175/BAMS-85-3-367, 2004.

Shao, Y. and Dong, C. H.: A Review on East Asian Dust Storm Climate, Modelling and Monitoring, *Global. Planet. Change*, 52, 1–22, 2006.

Shao, Y. and Lu, I.: A simple expression for wind erosion threshold friction velocity, *J. Geophys. Res.*, 105, 22437–22443, 2000.

20 Shao, Y. and Raupach, M.: Effect of saltation bombardment by wind, *J. Geophys. Res.*, 98, 12719–12726, 1993.

Shaw, G. E.: Transport of Asian Desert Aerosol to the Hawaiian Islands, *J. Appl. Meteorol.*, 19, 1254–1259, 1980.

25 Shimizu, A., Sugimoto, N., Matsui, I., Arai, K., Uno, I., Murayama, T., Kagawa, N., Aoki, K., Uchiyama, A., and Yamazaki, A.: Continuous observations of Asian dust and other aerosols by polarization lidars in China and Japan during ACE-Asia, *J. Geophys. Res.*, 109, D19S17, doi:10.1029/2002JD003253, 2004.

Shinn, E. A., Smith, J. M., Prospero, G. W., Betzer, P., Hayes, M. L., Garrison, V., and Barber, R. T.: African dust and the demise of Caribbean coral reefs, *Geophys. Res. Lett.*, 27, 3029–3032, 2000.

30 Smirnov, A., Holben, B. N., Savoie, D., Prospero, J. M., Kaufmann, Y. J., Tanré, D., Eck, T. F., and Slutsker, I. S.: Relationship between column aerosol optical thickness and in situ ground

- based dust concentrations over Barbados, *Geophys. Res. Lett.* 27, 1643–1646, 2000.
- Sokolik, I. and Toon, O. B.: Direct radiative forcing by anthropogenic airborne mineral aerosols. *Nature*, 381, 681–683, 1996.
- Sokolik, I. N. and Toon, O. B.: Incorporation of mineralogical composition into models of The radiative properties of mineral aerosol from UV to IR wavelengths, *J. Geophys. Res.* 104, 9423–9444, 1999.
- Stith, J. L., Ramanathan, V., Cooper, W. A., Roberts, G. C., DeMott, P. J., Carmichael, G., Hatch, C. D., Adhikary, B., Twohy, C. H., Rogers, D. C., Baumgardner, D., Prenni, A. J., Campos, T., Gao, R., Anderson, J., and Feng, Y.: An overview of aircraft observations from the Pacific Dust Experiment campaign, *J. Geophys. Res.*, 114, D05207, doi:10.1029/2008JD010924, 2009.
- Su, L. and Toon, O. B.: Numerical simulations of Asian dust storms using a coupled climate-aerosol microphysical model, *J. Geophys. Res.*, 114, D14202, doi:10.1029/2008JD010956, 2009.
- Tegen, I. and Fung, I.: Modeling of mineral dust in the atmosphere: Sources, transport, and Optical thickness, *J. Geophys. Res.*, 99, 22,897–22,914, 1994.
- Toon, O. B.: African dust in Florida clouds, *Nature*, 424, 623–624, 2003.
- Toon, O. B., Turco, R., Westphal, D., Malone, R., and Liu, M.: A multidimensional model for aerosols: Description of computational analogs, *J. Atmos. Science*, 45, 2123–2143, 1988.
- Tratt, D. M., Frouin, R. J., and Westphal, D. L.: April 1998 Asian dust event: A southern California perspective, *J. Geophys. Res.*, 106(D16), 18,371–18,379, 2001.
- Uno, I., Carmichael, G. R., Streets, D. G., Tang, Y., Yienger, J. J., Satake, S., Wang, Z., Woo, J., Guttikunda, S., Uematsu, M., Matsumoto, K., Tanimoto, H., Yoshioka, K., and Lida, T.: Regional chemical weather forecasting using CFORS: Analysis of surface observation at Japanese Island Station during the ACE-Asia experiment, *J. Geophys. Res.* 108(D23), 8668, doi:10.1029/2002JD002845, 2002.
- Uno, I., Satake, S., Carmichael, G. R., Tang, Y., Wang, Z., Takemura, T., Sugimoto, N., Shimizu, A., Murayama, T., Cahill, T. A., Cliff, S., Uematsu, M., Ohta., S., Quinn., P. K., and Bates, T. S.: Numerical study of Asian dust transport during the springtime of 2001 simulated with the Chemical Weather Forecasting System (CFORS) model, *J. Geophys. Res.*, 109, D19S24, doi:10.1029/2003JD004222, 2004.
- Uno, I., Harada, K., Satake, S., Hara, Y., and Wang, Z.: Meteorological Characteristics and dust distribution of the Tarim Basin simulated by the nesting RAMS/CFORS dust model, *J.*

Saharan and asian dust

L. Su and O. B. Toon

Title Page

Abstract

Introduction

Conclusions

References

Tables

Figures

◀

▶

◀

▶

Back

Close

Full Screen / Esc

Printer-friendly Version

Interactive Discussion



Saharan and asian dust

L. Su and O. B. Toon

Title Page

Abstract

Introduction

Conclusions

References

Tables

Figures

◀

▶

◀

▶

Back

Close

Full Screen / Esc

Printer-friendly Version

Interactive Discussion



Meteorol. Soc. Jpn., 83A, 219–239, 2005.

Uno, I., Yumimoto, K., Shimizu, A., Hara, Y., Sugimoto, N., Wang, Z., Liu, Z., and Winker, D. M.: 3D structure of Asian dust transport revealed by CALIPSO lidar and a 4DVAR dust model, *Geophys. Res. Lett.*, 35, L06803, doi:10.1029/2007GL032329, 2008.

5 Uno, I., Eguchi, K., Yumimoto, K., Takemura, T., Shimizu, A., Uematsu, M., Liu, Z., Wang, Z., Hara, Y., and Sugimoto, N.: Asian dust transported one full circuit around the globe, *Nat. Geosci.*, 2, 557–560, doi:10.1038/ngeo583, 2009.

VanCuren, R. A.: Asian aerosols in North America: Extracting the chemical composition and mass concentration of the Asian continental aerosol plume from long-term aerosol records in the western United States, *J. Geophys. Res.*, 108(D20), 4623, 16 pp., 2003.

10 Westphal, D. L., Toon, O. B., and Carlson, T. N.: A two-dimensional numerical investigation of the dynamics and microphysics of Saharan dust storms. *J. Geophys. Res.*, 92, 3027–3049, 1987.

Winker, D. M., Pelon, J. R., and McCormick, M. P.: The CALIPSO mission: Spaceborne lidar for observation of aerosols and clouds, *Proc. SPIE*, 4893, 1–11, 2003.

15 Winker, D. M., Hunt, W. H., and McGill, M. J.: Initial performance assessment of CALIOP, *Geophys. Res. Lett.*, 34, L19803, doi:10.1029/2007GL030135, 2007.

Wu, L.: Impact of Saharan air layer on hurricane peak intensity, *Geophys. Res. Lett.*, 34, L09802, doi:10.1029/2007GL029564, 2007.

20 Yin, Y., Levin, Z., Reisin, T. G., and Tzivion, S.: The effects of giant cloud condensation nuclei on the development of precipitation in convective clouds: A numerical study, *Atmos. Res.*, 53, 91–116, 2000.

Young, S., Winker, D., Vaughan, M., Hu, Y., Kuehn, R.: Extinction Retrieval Algorithms, CALIOP algorithm theoretical basis document PC-SCI-202 Part 4, available at: http://wwwcalipso.larc.nasa.gov/resources/calipso_users_guide/essential_reading/, 2008.

25 Zender, C. S., Huisheng, B., and Newman, D.: Mineral dust entrainment and Deposition (DEAD) model: Description and 1990s dust climatology. *J. Geophys. Res.*, 108(D14), 4416, 19 pp., 2003a.

Saharan and asian dust

L. Su and O. B. Toon

Title Page

Abstract

Introduction

Conclusions

References

Tables

Figures

◀

▶

◀

▶

Back

Close

Full Screen / Esc

Printer-friendly Version

Interactive Discussion



Table 1. The factors that contribute to the magnitudes of the total dust fluxes both for 2 Asian and Saharan dust simulated from the coupled CAM3.0/CARMA2.3 model in 2007. The % in the first two lines (wet and dry deposition) refers to the fraction of the dust 4 removed before traveling 45 degrees of longitude from the sources.

Impact factors (annual average)	Asian dust (total dust flux across source plane is 355 Tg in 2007)	Saharan dust (total dust flux across source plane is 1446 Tg in 2007)
Wet deposition	15%	10%
Dry deposition	75%	80%
Soil Erodibility Factor	0.077	0.081
Area of sources	$2.07 \times 10^6 \text{ km}^2$	$8.95 \times 10^6 \text{ km}^2$
Area lifting occurs	$1.33 \times 10^6 \text{ km}^2$	$4.17 \times 10^6 \text{ km}^2$
Power averaged wind	4.2 m/s	5.1 m/s
Soil moisture	$0.1 \text{ mm}^3/\text{mm}^3$	$0.03 \text{ mm}^3/\text{mm}^3$
Snow	$2.5 \times 10^{-5} \text{ mm/s}$	0

Saharan and asian dust

L. Su and O. B. Toon

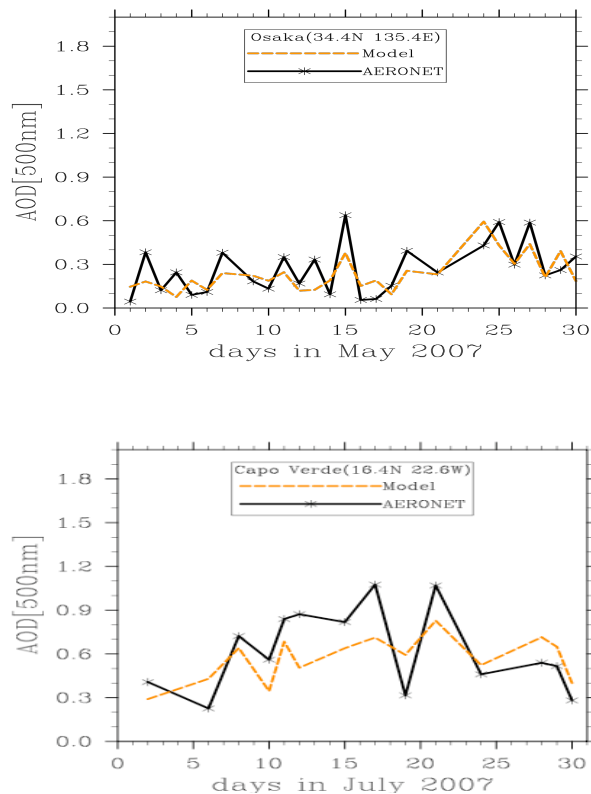


Fig. 1. The daily-averaged and column-integrated spectral optical depth (500 nm) at Osaka in May 2007 (top) and at Capo_Verde in July 2007 (bottom) 4 both from our model and from AERONET data.

[Title Page](#)[Abstract](#)[Introduction](#)[Conclusions](#)[References](#)[Tables](#)[Figures](#)[◀](#)[▶](#)[◀](#)[▶](#)[Back](#)[Close](#)[Full Screen / Esc](#)[Printer-friendly Version](#)[Interactive Discussion](#)

Saharan and asian dust

L. Su and O. B. Toon

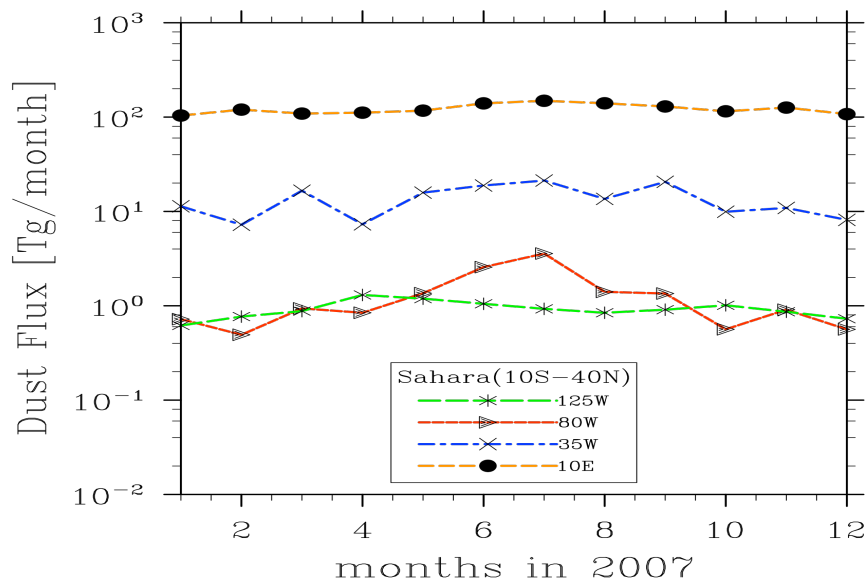


Fig. 2. Modeled monthly dust flux between 10° S–40° N, across different longitude planes (10° E, 35° W, 80° W, and 125° W) for Saharan dust in 2007.

[Title Page](#)[Abstract](#)[Introduction](#)[Conclusions](#)[References](#)[Tables](#)[Figures](#)[◀](#)[▶](#)[◀](#)[▶](#)[Back](#)[Close](#)[Full Screen / Esc](#)[Printer-friendly Version](#)[Interactive Discussion](#)

Saharan and asian dust

L. Su and O. B. Toon

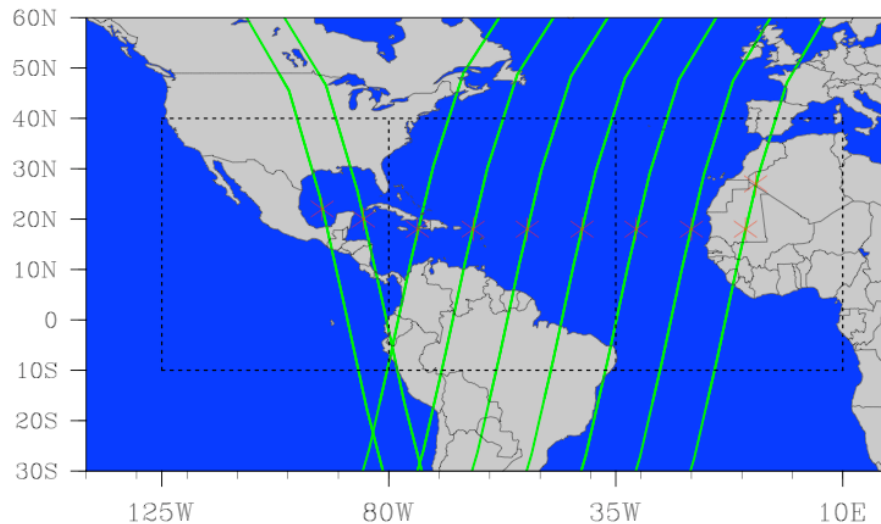


Fig. 3. Map used in this study for Saharan dust. The dashed lines denote the four longitude planes (10° E, 35° W, 80° W, and 125° W) and the latitude boundary (10° S to 40° N). The CALIPSO tracks are shown as lines along the asterisks.

[Title Page](#)[Abstract](#)[Introduction](#)[Conclusions](#)[References](#)[Tables](#)[Figures](#)[◀](#)[▶](#)[◀](#)[▶](#)[Back](#)[Close](#)[Full Screen / Esc](#)[Printer-friendly Version](#)[Interactive Discussion](#)

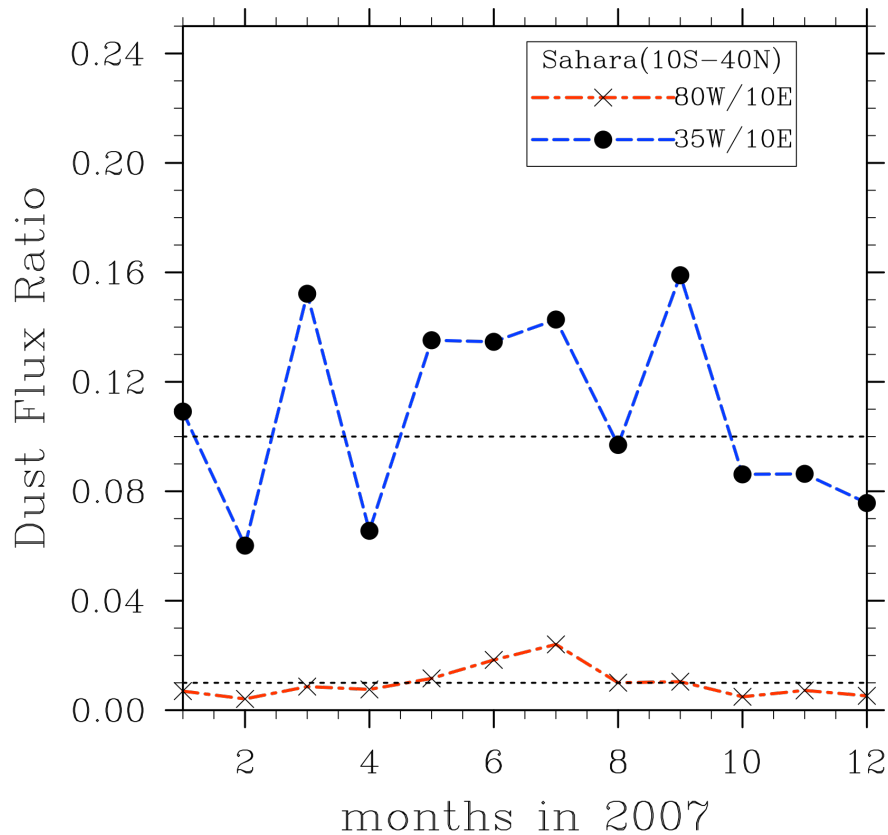


Fig. 4. Modeled monthly mean dust flux between 10° S to 40° N. The asterisk- marked line denotes the ratio of the flux as 80° W to that at 10° E, and the blue dashed-line denotes the ratio of the flux at 35° W to that at 10° E for Saharan dust in 2007. The dashed lines mark 0.1 and 0.01.

Saharan and asian dust

L. Su and O. B. Toon

Title Page

Abstract Introduction

Conclusions References

Tables Figures

◀ ▶

◀ ▶

Back Close

Full Screen / Esc

Printer-friendly Version

Interactive Discussion



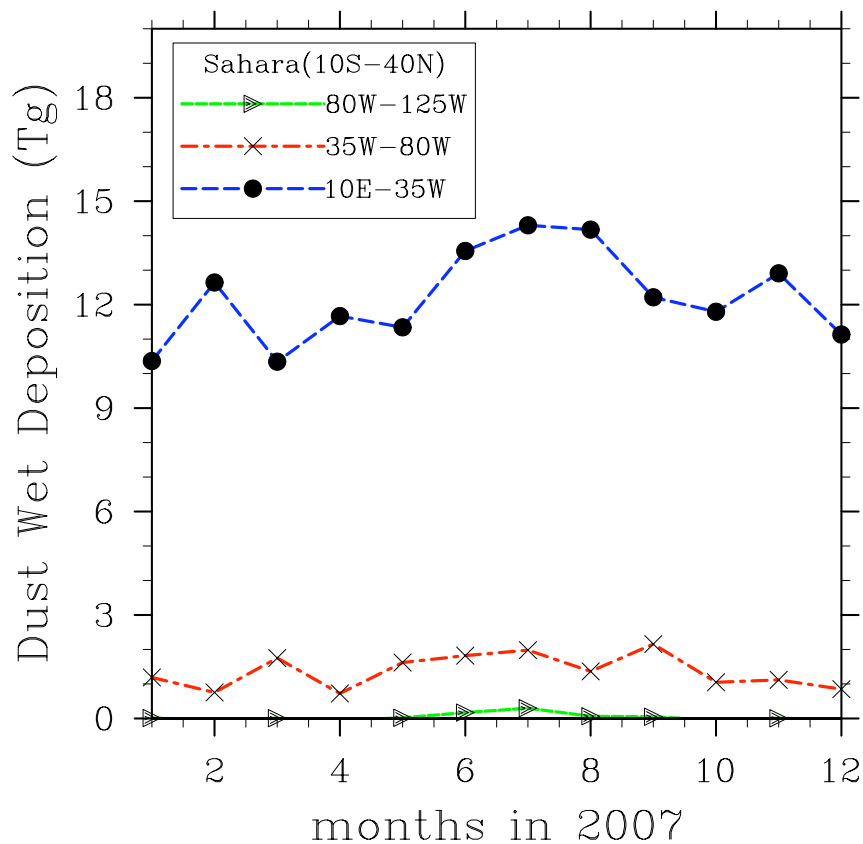


Fig. 5. Modeled monthly dust wet deposition between 10° S to 40° N for longitudes between 10° E to 35° W, 35° W– 80° W, and 80° W– 125° W for Saharan dust in 2007.

Saharan and asian dust

L. Su and O. B. Toon

Title Page

Abstract Introduction

Conclusions References

Tables Figures

◀ ▶

◀ ▶

Back Close

Full Screen / Esc

Printer-friendly Version

Interactive Discussion



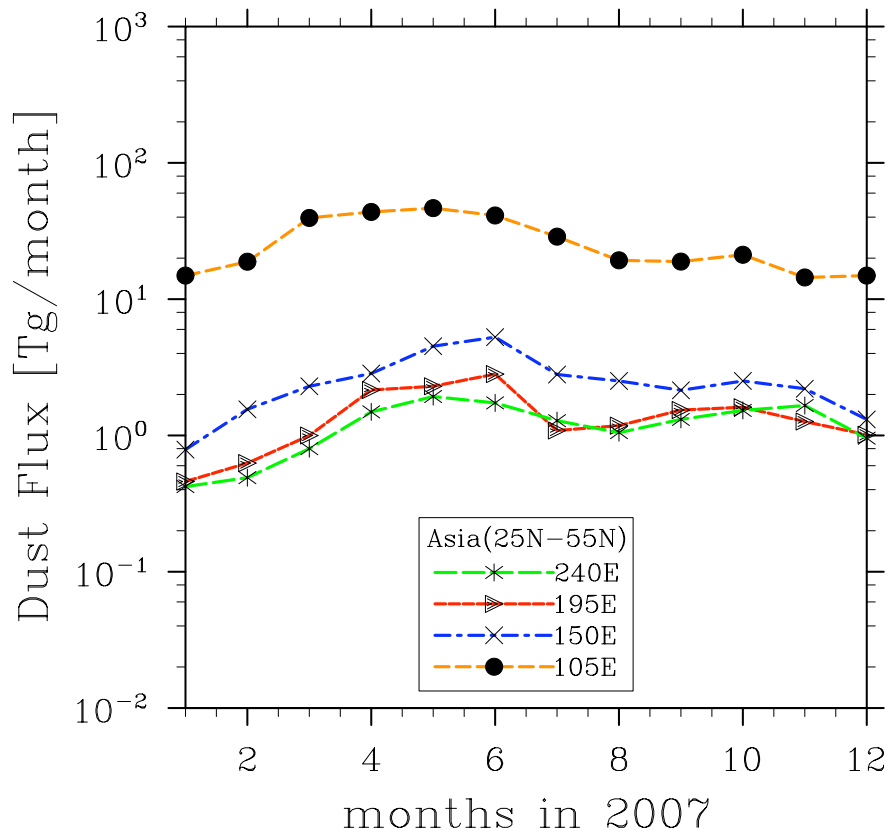


Fig. 6. Modeled monthly dust wet deposition between 10° S to 40° N for longitudes between 10° E to 35° W, 35° W–80° W, and 80° W–125° W for Saharan dust in Modeled monthly dust fluxes (25° N–55° N) across different longitude planes (105° E, 150° E, 195° E, and 240° E) for Asian dust in 2007.

Saharan and asian dust

L. Su and O. B. Toon

Title Page

Abstract Introduction

Conclusions References

Tables Figures

◀ ▶

◀ ▶

Back Close

Full Screen / Esc

Printer-friendly Version

Interactive Discussion



Saharan and asian dust

L. Su and O. B. Toon

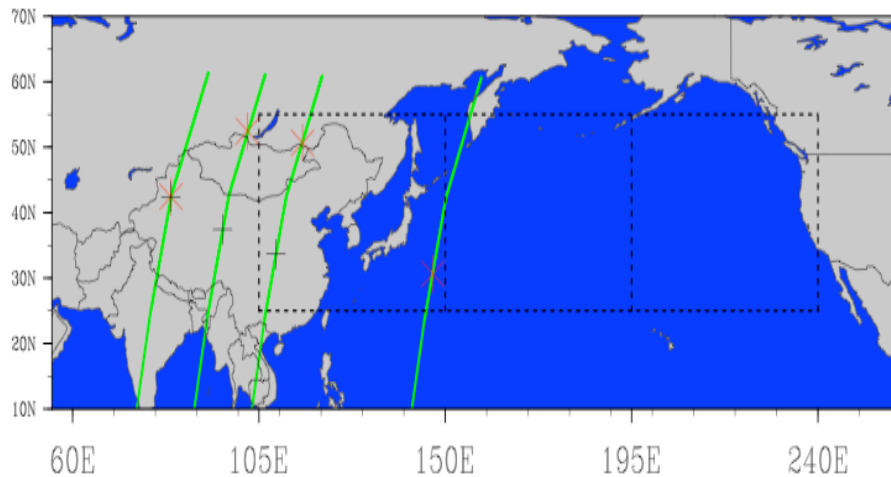


Fig. 7. Map used in this study for Asian dust. The dashed lines denote the four longitude planes (105° E, 150° E, 195° E, and 240° E) and the latitude boundary (25° N to 55° N). The CALIPSO tracks are shown as lines along the asterisks and cross marks.

[Title Page](#)[Abstract](#)[Introduction](#)[Conclusions](#)[References](#)[Tables](#)[Figures](#)[I◀](#)[▶I](#)[◀](#)[▶](#)[Back](#)[Close](#)[Full Screen / Esc](#)[Printer-friendly Version](#)[Interactive Discussion](#)

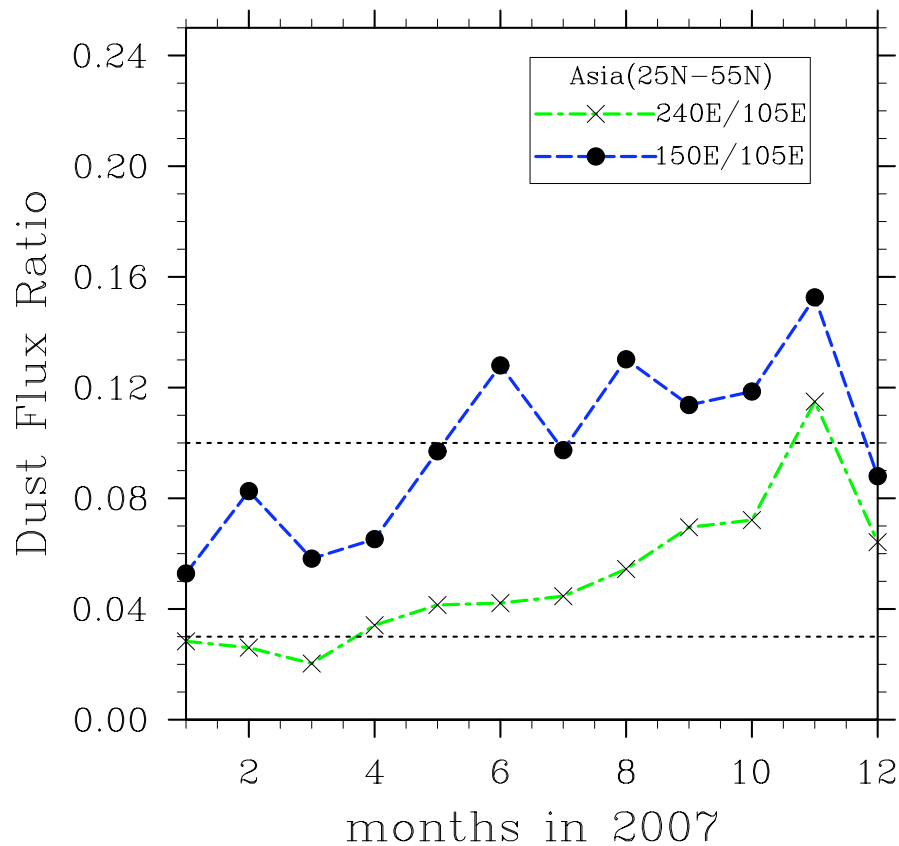


Fig. 8. Modeled ratios of monthly dust flux between 25° N to 55° N for Asian dust in 2007. The horizontal dashed lines are the 0.1 and 0.03 lines.

Saharan and asian dust

L. Su and O. B. Toon

Title Page

Abstract Introduction

Conclusions References

Tables Figures

◀ ▶

◀ ▶

Back Close

Full Screen / Esc

Printer-friendly Version

Interactive Discussion



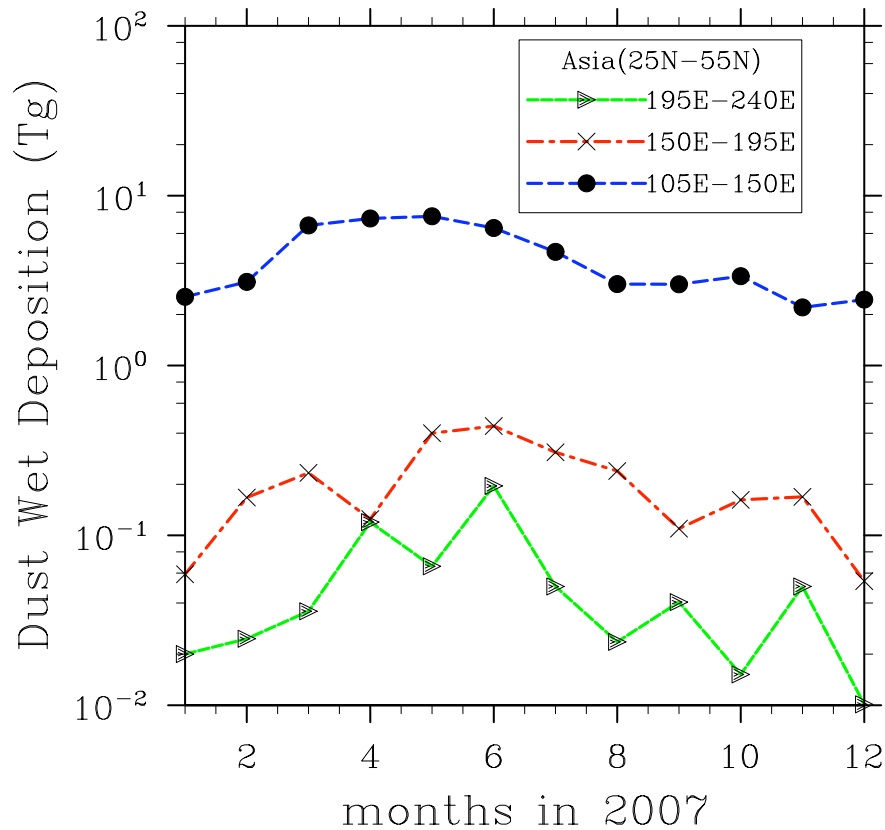


Fig. 9. Modeled ratios of monthly dust flux between 25° N to 55° N for Asian 3 dust in 2007. The horizontal dashed lines are the 0.1 and 0.03 lines. Modeled monthly dust wet deposition between 25° N to 55° N for regions between 105° E to 150° E, 150° E to 195° E, and 195° E to 240° E for Asian dust in 2007.

Saharan and asian dust

L. Su and O. B. Toon

Title Page

Abstract Introduction

Conclusions References

Tables Figures

◀ ▶

◀ ▶

Back Close

Full Screen / Esc

Printer-friendly Version

Interactive Discussion



Saharan and asian dust

L. Su and O. B. Toon

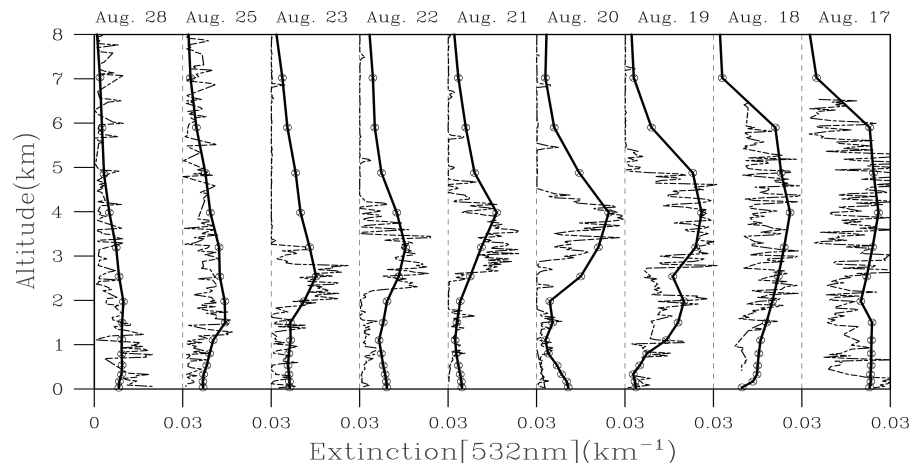


Fig. 10. Modeled ratios of monthly dust flux between 25° N to 55° N for Asian 3 dust in 2007. The horizontal dashed lines are the 0.1 and 0.03 lines. Modeled monthly dust wet deposition between 25° N to 55° N for regions between 105° E to 150° E, 150° E to 195° E, and 195° E to 240° E for Asian dust in 2007. Comparison of vertical distribution of Saharan dust between model simulations and CALIPSO observations in August of 2006.

Title Page

Abstract

Introduction

Conclusions

References

Tables

Figures

◀

▶

◀

▶

Back

Close

Full Screen / Esc

Printer-friendly Version

Interactive Discussion



Saharan and asian dust

L. Su and O. B. Toon

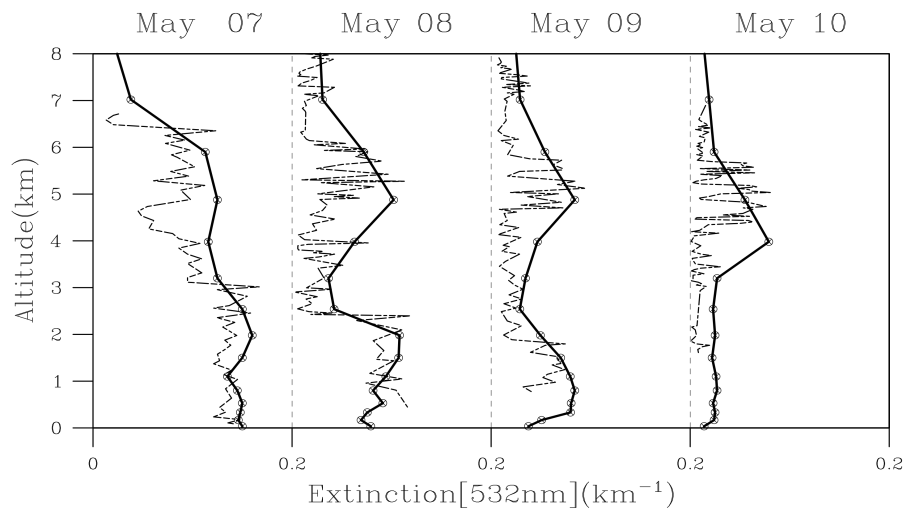


Fig. 11. Comparison of vertical distribution of Asian dust between model simulations and CALIPSO observations in May of 2007.

[Title Page](#)[Abstract](#)[Introduction](#)[Conclusions](#)[References](#)[Tables](#)[Figures](#)[◀](#)[▶](#)[◀](#)[▶](#)[Back](#)[Close](#)[Full Screen / Esc](#)[Printer-friendly Version](#)[Interactive Discussion](#)

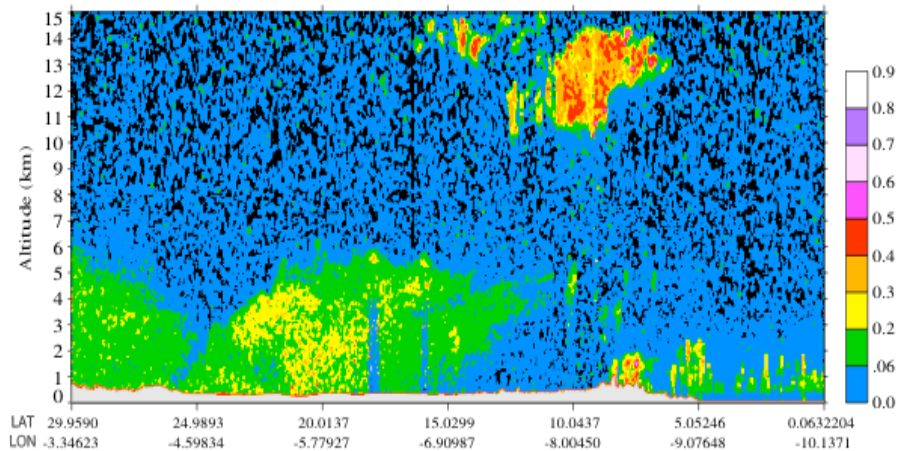


Fig. 12. The 532-nm depolarization ratio for Saharan dust on 21 July 2007.

Saharan and asian dust

L. Su and O. B. Toon

Title Page	
Abstract	Introduction
Conclusions	References
Tables	Figures
◀	▶
◀	▶
Back	Close
Full Screen / Esc	
Printer-friendly Version	
Interactive Discussion	



Saharan and asian dust

L. Su and O. B. Toon

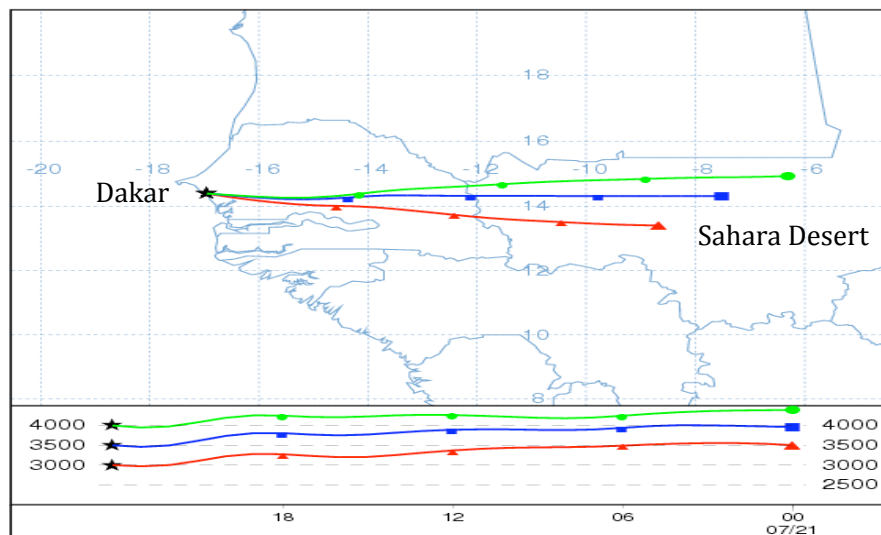


Fig. 13. Back trajectory of Sahara dust in Dakar on 21 July 2007 using 3 HYSPLIT model for three altitudes: 3000 m (red curve), 3500 m (blue 4 curve), and 4000 m (green curve). The horizontal trajectory components 5 (top) and the vertical components (bottom) are shown in the figure.

[Title Page](#)[Abstract](#)[Introduction](#)[Conclusions](#)[References](#)[Tables](#)[Figures](#)[I◀](#)[▶I](#)[◀](#)[▶](#)[Back](#)[Close](#)[Full Screen / Esc](#)[Printer-friendly Version](#)[Interactive Discussion](#)

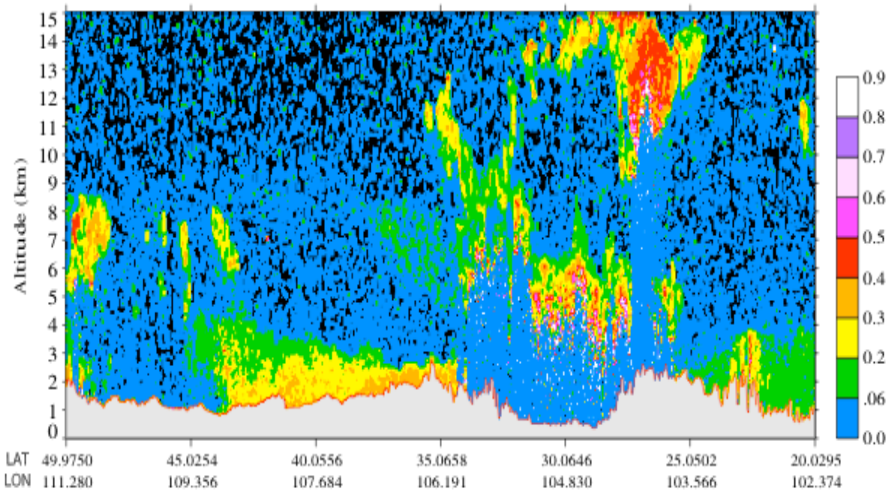


Fig. 14. The 532-nm depolarization ratio for Asian dust on 23 May 2007.

Saharan and asian dust

L. Su and O. B. Toon

Title Page	
Abstract	Introduction
Conclusions	References
Tables	Figures
◀	▶
◀	▶
Back	Close
Full Screen / Esc	
Printer-friendly Version	
Interactive Discussion	



Saharan and asian dust

L. Su and O. B. Toon

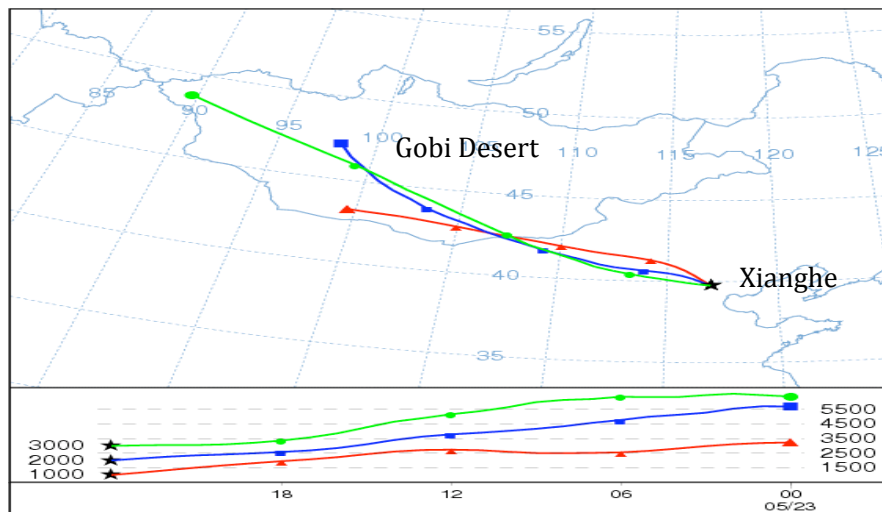


Fig. 15. Back trajectory of Asian dust in Xianghe on 23 May 2007 using HYSPLIT model for three altitudes: 1000 m (red curve), 2000 m (blue curve), and 3000 m (green curve). The horizontal trajectory components (top) and the vertical components (bottom) are shown in the figure.

Title Page

Abstract

Introduction

Conclusions

References

Tables

Figures

◀

▶

◀

▶

Back

Close

Full Screen / Esc

Printer-friendly Version

Interactive Discussion



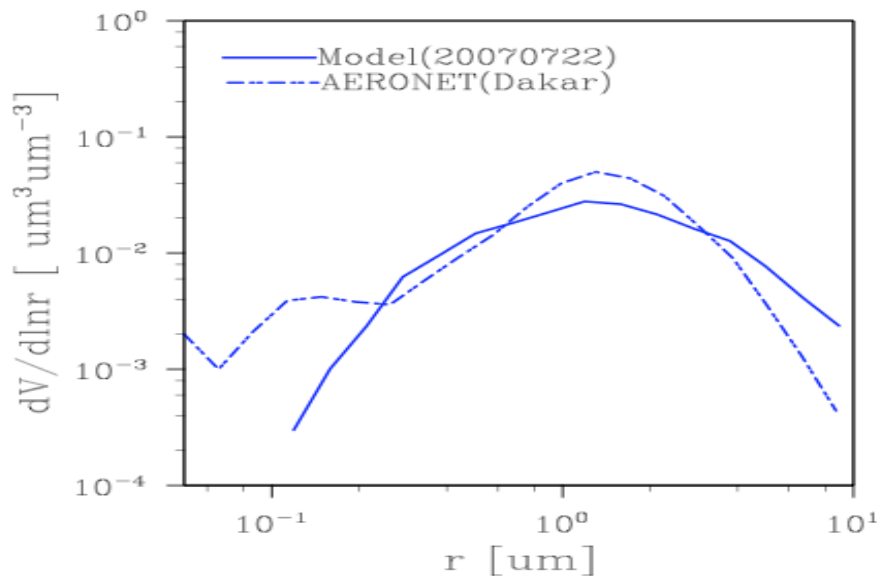


Fig. 16. Modeled volume size distribution of Saharan dust in Dakar (14.39° N , 16.95° W) constrained by AERONET measurements.

Saharan and asian dust

L. Su and O. B. Toon

Title Page

Abstract Introduction

Conclusions References

Tables Figures

◀ ▶

◀ ▶

Back Close

Full Screen / Esc

Printer-friendly Version

Interactive Discussion



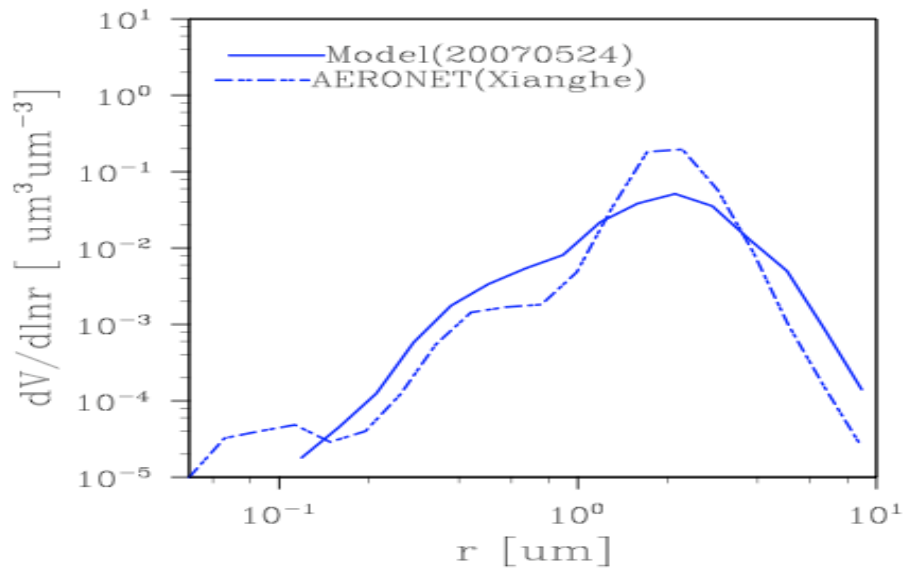


Fig. 17. Modeled volume size distribution of Saharan dust in Dakar (14.39° N, 16.95° W) constrained by AERONET measurements. Modeled volume size distribution of Asian dust in Xianghe (39.75° N, 116.96° E) constrained by AERONET measurements.

Saharan and asian dust

L. Su and O. B. Toon

Title Page

Abstract Introduction

Conclusions References

Tables Figures

◀ ▶

◀ ▶

Back Close

Full Screen / Esc

Printer-friendly Version

Interactive Discussion



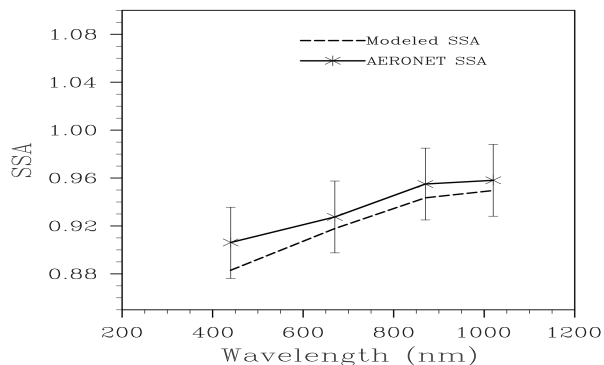
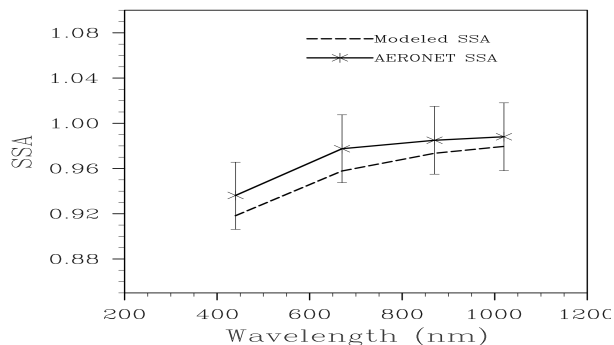


Fig. 18. Modeled volume size distribution of Saharan dust in Dakar (14.39° N , 16.95° W) constrained by AERONET measurements. Modeled volume size distribution of Asian dust in Xi-anqhe (39.75° N , 116.96° E) constrained by AERONET measurements. The comparison of the single scattering albedo between the model simulations and the AERONET retrievals both for Asia Deserts (top) (Dalanzadgad (43.3° N , 104.3° E) in April 2006) and Sahara Deserts (bottom) (Tamanrasset_TMP (22.5° N , 5.3° E) in July 2006).